Defining a 3-Dimensional (3D) *in vitro* model to study Immune Cell and Renal Cell interactions

SADIA AFRIN

Submitted in fulfilment of the requirements for the degree of
Master of Applied Science (Research)

Chemistry, Physics and Mechanical Engineering School
Faculty of Science and Engineering
Queensland University of Technology
2015

KEYWORDS

3D *in vitro* model

Hydrogels

Immune modulation

Proximal tubule epithelial cells

T lymphocytes

ABSTRACT

Background. The incidence rate of Chronic Kidney Disease (CKD) in Australia is rising rapidly. CKD leads to end stage kidney disease and the cost of treating the condition from 2009 to 2020 is estimated to account for $12 billion to the Australian health care system. At earlier stages of the disease, when the kidneys are not yet substantially damaged, proximal tubule epithelial cells (PTEC) of the kidney may play a very critical role in reducing extent of damage to kidneys and limit progression to CKD. PTEC are known to respond to and contribute to the pathological process in a range of kidney diseases. PTEC have been isolated and cultured along with purified immune cells and their interactions studied in simple 2-dimensional (2D) allogeneic cell culture model and mouse models. More recently, using a 2D culture model it has been shown that PTEC are able to modulate the immune response in an autologous human system. However, 3D culture models would enable such immune modulatory processes to be studied within a more physiologically relevant setting. Therefore we aimed to recapitulate the PTEC/immune cell niche by developing a 3D hydrogel system in which PTEC and purified T cells could be cultured together and their interactions monitored using different techniques.

Methods. The overall goal was to develop a 3D hydrogel system for the co-culture of PTEC and purified populations of immune cells, which would enable the study of the immunomodulatory function of PTEC within a more representative *in vivo* environment. The first step was maintaining viability and *in vivo* morphology of purified immune cells and PTEC within a suitable hydrogel. To determine cell viability and morphology, the cells were stained within the gels with fluorescein diacetate (viable cells) and propidium iodide (dead cells). Images were taken with a confocal microscope. Immune cell functions were investigated by analysing the expression of classical antigen presenting and co-stimulatory molecules using flow cytometry. Protocols for gel dissolution were established to recover the immune cells and the PTEC from the hydrogel for analysis by flow cytometry. Part of the work also involved defining the chemokines secreted by PTEC under inflammatory

conditions, which are responsible for the migration of T cells in 2D cultures and through the extracellular matrix (ECM) in 3D gel systems. A human chemokine kit based on the cytokine bead array platform was used for this purpose. To determine whether activated PTEC modulate responses of the autologous immune cells via their expression of activation/maturation Ags, up-regulation of cell surface markers were analysed with direct immunofluorescent staining with specific antibodies.

Results. Data suggested that PTEC and T cells remain viable in type I collagen hydrogels for at least 7 days. Both PTEC and T cells were able to migrate and interact with each other when embedded in collagen gels. In collagen hydrogels T cells up-regulated activation markers CD25 and CD69, following mitogen stimulation, to similar levels as those in 2D cultures. Importantly, within these 3D gels, PTEC were able to more effectively down-modulate T cell responses than within 2D cultures. PTEC within these gels produced a range of chemokines including RANTES, IP-10, IL-8, MCP-1 and MIG.

TABLE OF CONTENTS

LIST OF FIGURES

LIST OF TABLES

LIST OF ABBREVIATIONS

1MT	1 methyl-D-tryptophan
2D	2-dimensional
3D	3-dimensional
Ab	Antibody
Ag	Antigen
APC	Antigen presenting cell
BSA	Bovine Serum Albumin
C	Celsius
CBA	Cytokine Bead Array
CD	Cluster of differentiation
CFSE	Carboxyfluorescein Diacetate Succinimidyl Ester
cGy	CentiGray
CKD	Chronic kidney disease
CM	Complete media
cpm	Counts per minute
CTL	Cytotoxic T cell
CVD	Cardiovascular disease
DAPI	4’,6-diamidino-2-phenylindole

DC	Dendritic cell
DM	Defined media
DMEM	Dulbecco's modified Eagle's medium
DMSO	Dimethyl sulfoxide
ECM	Extracellular matrix
EDTA	Ethylene diamine tetra-acetic acid
EGF	Epidermal growth factor
EHS	Engelbreth-Holm-Swarm
ESRD	End stage renal disease
FACS	Fluorescence-activated cell sorting
FDA	Fluorescein diacetate
FGF	Fibroblast growth factor
GAS	Interferon-gamma activated sequence
GDL	D-(+)-Gluconic acid δ lactone
GelMA	Gelatin-methacrylamide
GFR	Glomerular filtration rate
GFR	Growth factor-reduced
HEPES	N-2-hydroxyethylpiperazine-N'-2-ethanesulfonic acid
HK-2	Human kidney-2
HLA-DR	Human leukocyte antigen –DR
HUVEC	Human umbilical vein endothelial cells
ICOS-L	Inducible T-cell co-stimulator ligand
IDO	Indoleamine 2, 3-dioxygenase
IFN- γ	Gamma- interferon
IFNGR	IFN-γ-receptor
IFN-α	Alpha-interferon

IGF	Insulin-like growth factor
IgG	Immunoglobulin
IL	Interleukin
IP-10	Interferon gamma-induced protein 10
ISRE	Interferon-stimulated response element
MACS	Magnetic activated cell sorting
MCP-1	Monocyte chemotactic protein-1
MDCK	Madin-Darby Canine Kidney
MEK	Mouse embryonic kidney
MFI	Mean fluorescence intensity
Mg^{2+}	Magnesium ions
MHC-I	Major histocompatibility class I
MHC-II	Major histocompatibility class II
MIG	Monokine induced by gamma interferon
MSC	Mesenchymal stem cells
NaOH	Sodium Hydroxide
Near-IR	Near –Infrared
NKT	Natural Killer T cells
PBMC	Peripheral blood mononuclear cells
PBS	Dulbecco's Phosphate Buffered Saline
PDGF	Platelet derived growth factor
PD-L1	Programmed death-ligand 1
PFA	Paraformaldehyde
PHA	Phytohaemagglutinin
PI	Photo Initiator (Irgacure 2959) [2-hydroxy-1-[4-(2-hydroxyethoxy) phenyl]-2-methyl-1-propanone] (Irgacure 2959)

PI	Propidium Iodide
PNA	Peanut agglutinin
PTEC	Proximal tubule epithelial cells
RANTES	Regulated upon activation normal T-cell expressed and secreted
RPMI-1640	Roswell Park Memorial Institute medium 1640
RRT	Renal replacement therapy
Stat1α	Signal transducer, activator of transcription 1 α
TCR	T – cell antigen receptor
TGF-β	transforming growth factor beta
T_h	T helper cells
TNF-α	Tumor necrosis factor –alpha
T_{reg}	Regulatory T cells
VIC	Aortic valvular interstitial cells

Statement of Original Authorship

The work contained in this thesis has not been previously submitted to meet requirements for an award at this or any other higher education institution. To the best of my knowledge and belief, the thesis contains no material previously published or written by another person except where due reference is made.

QUT Verified Signature

Signature:

Date: 05-June-2015

Works for publication by the Author incorporated into the Thesis

In preparation

1. Afrin S, Klein T J, Schrobback K, Kassianos A J, Wang X, Healy H, Wilkinson R . Defining A 3-Dimensional (D) *in vitro* Model To Study Immune Cell And Renal Cell Interactions**.**

Additional Published Works by the Author Relevant to the Thesis but not Forming Part of it

Paper in press for publication

1. Kassianos A, Wang X, Sampangi S**, Afrin S,** Wilkinson R, Healy H. **Fractalkine-CX3CR1-dependent recruitment and retention of human CD1c+ myeloid dendritic cells by in vitro activated proximal tubular epithelial cells. Kidney Int. 2015 Jan 14. doi: 10.1038/ki.2014.407. [Epub ahead of print].**

2. Sampangi S, Wang X, Beagley K**, Afrin S**, Klein T, Healy H, Wilkinson R, Kassianos A. **Human proximal tubule epithelial cells (PTEC) modulate autologous B cell function. Nephrology Dialysis Transplantation. Accepted May 2015**

3. Sandeep Sampangi1, Andrew J Kassianos, Xiangju Wang, Kenneth W Beagley, Travis Klein, **Sadia Afrin**, Helen Healy and Ray Wilkinson. **The mechanisms of human renal epithelial cell modulation of autologous dendritic cell phenotype and function. Submitted**

Poster presentations:

1. **Sadia Afrin**, Ray Wilkinson, Travis J. Klein, Karsten Schrobback, Andrew J Kassianos, Xiangju Wang, Helen Healy. Defining a 3-Dimensional (D) *in vitro* model to study immune cell- renal cell interactions. Brisbane Immunology Group (BIG) August 2013.
2. **Afrin, Sadia**, Schrobback, Karsten, Kassianos, Andrew J., Wang, Xiangju, Healy, Helen, Wilkinson, Ray, Klein, Travis J. Defining a 3-Dimensional (D) *in vitro* model to study immune-renal cell interactions. IHBI Inspires, Brisbane, November 2013.
3. **Afrin S**, Wilkinson R, Klein T J, Schrobback K, Kassianos A J, Wang X, Healy H. Defining A 3-Dimensional (D) *in vitro* Model To Study Immune Cell And Renal Cell Interactions. 23 rd RBWH Symposium, Brisbane, October 2014.
4. R Wilkinson, AJ Kassianos, X Wang, S Sampangi, **S Afrin** and H Healy. Fractalkine-CX3CR1-dependent recruitment and retention of TGF-β-producing $CD1c^+$ myeloid dendritic cells in human kidney disease. 13th International symposium on Dendritic Cells, France, September 2014.
5. Sandeep Sampangi, Andrew Kassianos, Xiangju Wang, **Sadia Afrin**, Ray Wilkinson and Helen Healy. B cell function is modulated by autologous human kidney proximal tubule epithelial cells (PTEC). 23rd RBWH Symposium, Brisbane, October 2014.
6. Healy H, Sampangi S, Kassianos A, Wang X, **Afrin S**, Wilkinson R. Human PTEC modulate autologous B cell function. American Society of Nephrology (ASN) meeting, Philadelphia, U.S.A. To be presented in November 2014.

ACKNOWLEDGEMENTS

I would like to offer my gratitude to my supervisors A/Prof Ray Wilkinson, A/Prof Travis Klein and Dr. Karsten Schrobback for their invaluable support and guidance during the tenure of my candidature. I am grateful to them for providing me with insightful suggestions without which this work would not have been possible.

I greatly appreciate the assistance and help provided by Andrew, Annie and Sandeep for the experimental work and data analysis required to complete this thesis. I would also like to extend my sincere thanks to A/Prof Travis Klein for providing financial support during my masters.

The encouragement and kindness from A/Prof Ray Wilkinson will always be remembered. I sincerely appreciate his help and support throughout my candidature.

Last but not least I am grateful to my family - Tanveer and Arissa for being understanding and a constant source of inspiration in my life.

Chapter 1: Introduction

1.1. Background

Chronic Kidney Disease (CKD) is a common chronic disease in Australia that is increasing at an alarming rate. CKD is usually asymptomatic and detected at later stages of the disease when substantial damage to the kidneys has already occurred. The disease often leads to a broad range of complications, such as hypertension, anaemia, malnutrition, bone disease, neuropathy, and decreased quality of life. End stage renal disease (ESRD) is reached when the glomerular filtration rate (GFR) falls below 15 mL/min per 1.72 m^2 and patients need renal replacement therapy (RRT) or kidney transplant to survive. In Australia the incidence rate of treated ESRD is projected to increase by nearly 80 %—from 11 per 100,000 populations in 2009 to 19 per 100,000 populations in 2020. This increase is anticipated to be mainly among patients aged 70 years and over (The Australian Institute of Health and Welfare, AIHW) [1]. As the incidence rate increases, the costs of treating end-stage kidney disease from 2009 to 2020 would account for $12 billion to the Australian health care system [2].

It is well accepted that regardless of the primary insult in kidneys, damage of the tubular epithelial cells and interstitium leads to renal dysfunction. During earlier stages of the disease, proximal tubule epithelial cells (PTEC) of the kidneys play an important role in recruiting inflammatory immune cells into the kidney interstitium. Previous published studies from the Conjoint Renal Medicine Laboratory at Queensland Institute of Medical Research (QIMR) Berghofer have shown that in 2-dimensional (2D) cultures, primary human PTEC are able to modulate the functions of autologous immune cells, possibly to reduce the degree of damage that can occur to kidney tubules during inflammation [3].

The cellular microenvironment or extracellular matrix (ECM) is known to influence cell behaviour and function. It is evident from research that the ECM composition is able to control the fate of a cell. Cell matrix properties highly influence cell adhesion, migration and also cell signalling [4]. In kidneys, the cellular microenvironment is recognised to be correlated to renal function [5]. Therefore, we

hypothesized that a 3-dimensional (3D) *in vitro* model would more closely resemble the *in vivo* physiological conditions and provide the opportunity for the kidney cells and immune cells to exhibit their typical phenotype and functionality.

The context of this thesis was to define a 3D environment for PTEC and immune cells as opposed to a conventional 2D culture. The investigation also included analysing the action of molecules involved in interactions between these two types of cells under a more physiological environment. The broader objective of developing a relevant 3D model of immune-renal cell interactions was to define molecules that could be targeted for use as therapeutics at earlier stages of CKD to prevent or ameliorate most of the complications of decreased renal function, as well as delay the progression to kidney failure.

1.2. Purposes

This thesis aimed to establish suitable 3D matrix systems for co-culture of PTEC and immune cells. Further, it aimed to recover cells and analyse changes in surface antigen expression by manipulating the physical and chemical properties of different 3D hydrogel systems. The results obtained from the 3D culture were compared with studies that were carried out using the traditional 2D culture system. Hence, this study sought to prove that *in vivo* -like organization of cells within gel constructs elicited more relevant and reliable interactions compared to 2D cell cultures. The use of multiple cell types in this model was critical in creating a more *in vivo* -like organization of the cells and observing appropriate cell physiological responses.

1.3. Significance and Scope

PTEC have previously been isolated and cultured along with purified immune cells and their interactions studied using traditional 2D culture. As most research involves 2D experimental systems, little is actually known about what occurs in a 3D environment. Therefore, this thesis seeks to fill this gap of knowledge by investigating the influence of a more physiologically relevant 3D model on the interaction of these two types of cells. In kidney research, the use of 3D models is not widespread and mainly limited to organ or organoid cultures. To overcome the

hurdles of these complex techniques, in this thesis a matrix made of a suitable hydrogel is defined to co-culture kidney and immune cells.

This thesis was completed with the collaborative effort of the Cartilage Regeneration Laboratory (CRL) at IHBI, QUT, and the Conjoint Renal Medicine Laboratory at QIMR Berghofer. CRL has been working with 3D culture systems involving chondrocytes, bone marrow derived mesenchymal stem cells (MSCs), fibroblasts and a number of hydrogels [6, 7]. The Conjoint Renal Medicine Laboratory has previously studied autologous immune cell – renal cell interactions in 2D cultures. Now, in a collaborative effort, this thesis defines a 3-D *in vitro* model to study immune cell – renal cell interactions. This model would enable us to gain novel insights into immune modulations of PTEC on the autologous immune cells in an environment more closely resembling that of native tissue.

1.4. Hypotheses and Aims

The overall goal of the project was to develop a 3D hydrogel system for the co-culture of PTEC and purified populations of immune cells, to enable the study of the immunomodulatory function of PTEC within a more representative *in vivo* environment. To reach this goal, the project had the following specific aims:

AIM 1: Define a suitable hydrogel capable of maintaining viability and function of purified T cells and autologous PTEC within the hydrogel;

To construct a versatile model for the co-culture of primary PTEC and T cells, different types of hydrogels were studied. Biomaterials that closely resemble the native ECM and would allow the cells to exhibit a physiologically relevant phenotype were examined in this thesis. Suitability of gels were analysed by determining viability of the cells within the gels. Morphology and ability of the cells to interact within the defined 3D model were examined by live-cell imaging using a confocal microscope.

AIM 2: Develop techniques for recovery of the immune cells and the PTEC from the hydrogel for analysis.

For the purposes of this study it was vitally important to not only identify a suitable gel matrix for both PTEC and immune cells but also to be able to dissociate these cells from the gel matrix and analyse their phenotypic and functional characteristics. The immune cells and PTEC were recovered from the gel system after being cultured for 6 days to determine their immunomodulatory functions. This recovery was achieved by dissolution of the gel constructs enzymatically or through the removal of calcium ions with chelating agents, such as EDTA or citric acid. A suitable chelator or enzyme and its concentration were optimised experimentally as these may affect the presentation of certain cell surface antigens (Ag).

AIM 3: Monitor the immunomodulatory function of PTEC in the defined model system.

Immune modulation by PTEC was determined by parameters such as expression of classical antigen presenting and co-stimulatory molecules. Interactions between PTEC and the immune cells within the 3D model were visualized by live cell microscopy. Effector T cell responses and cytokine secretion were analysed using flow cytometry and Cytometric Bead Array (CBA) respectively. The results obtained from 3D gel system were compared with 2D cell culture.

Chapter 2: Literature Review

2.1. Kidney Anatomy and Physiology:

2.1.1. Kidney structure and function

Kidneys are bean-shaped organs located towards the back of the abdominal cavity which play numerous vital roles in the body including the excretion of wastes like urea and ammonium, maintaining acid-base balance, re-absorption of important substances (e.g. water, glucose, amino acids) and production of hormones including calcitriol, erythropoietin, and the enzyme renin. Kidneys also play a vital role in regulating blood pressure.

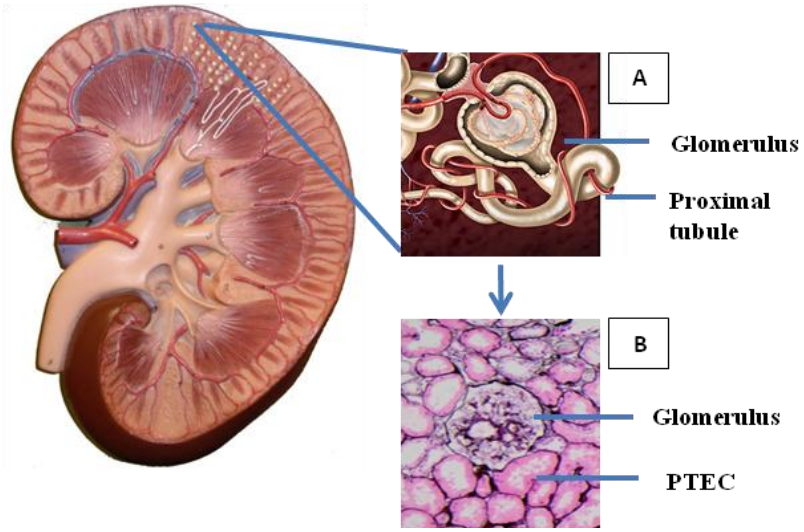

Figure 2.1 Cross section of a kidney (A) showing the nephron (B) Stained kidney tissue showing the glomerulus and proximal tubule epithelial cells (PTEC). (adapted from R.Wilkinson, Frontiers in Immunological Research presentation, Salzburg 2012).

The kidney is segmented into an inner section, called the medulla, and an outer section, called the cortex. The cortex contains approximately one million nephrons, which are the functional units of the kidney (**Figure 2.1**). Each nephron comprises of a network of capillary loops called the glomerulus, which is housed within the fluid filled Bowman's capsule and a complex ductal system. The Bowman's capsule extends into the duct system beginning with the proximal convoluted tubule, which is followed by the Loop of Henle and the distal convoluted tubule that finally drains into a collecting duct. Each region of the duct

system is distinct and differs in structure, function and morphology. The collecting ducts lead to the ureter, which drains urine into the urinary bladder.

The prime function of the proximal tubule is re-absorption of water, small proteins, amino acids, carbohydrates and electrolytes, whilst acid-base balance is partially regulated by both the proximal and distal tubule [8].

The kidney is comprised of distinct cell types. The glomerulus and the Bowman's capsule consist of podocytes, mesangial cells and parietal cells. The glomerulus is lined by parietal cells and contains the mesangium that supports a network of blood capillaries. Blood is filtered through the glomerular filtration barrier. The barrier consists of endothelial cells, a basement membrane and podocytes. Molecules below 68kDa pass through the filter barrier to enter a duct system [9]. Juxtaglomerular cells and parietal cells together form the Bowman's capsule. Parietal cells protect the glomeruli and the juxtaglomerular cells release the hormone renin which functions to regulate blood pressure. The proximal and distal convoluted tubules are both lined with columnar epithelial cells that differ in appearance. Distal tubule cells are shorter, whereas PTEC are of greater columnar height and have brush borders which contain numerous megalin and cubilin receptors. Molecules that are not reabsorbed by the tubular system form the urine. The space between the tubules is called the interstitium and it is here where most of the intra-renal immune cells are found [8, 9].

2.1.2. Kidney resident immune cells

A range of immune cell populations have been reported within a normal kidney. Macrophages lie adjacent to the basement membrane of PTEC in the outer medulla whereas dendritic cells (DC) are found in abundance in the tubulointerstitium. No DCs are found in the glomeruli .This strict localisation and strategic placement of DC is suggested to be optimal for antigen capture. Macrophages found in the medulla are believed to take part in homeostasis and repair mechanisms [9]. Monocytes are mostly present in the glomerular region of the kidneys [10, 11]. An infiltration of leukocytes from the surrounding blood capillaries occurs under perturbed disease states.

2.1.3. The role of extracellular matrix

Extracellular matrix (ECM) may be described as a three-dimensional framework of structural and functional proteins that not only provides physical support to the cells for their spatial organization but also regulates cell growth and proliferation by interacting with various growth factors. Research has shown that during kidney development and repair

processes, ECM molecules and their receptors play a crucial and dynamic role in providing an architectural scaffold for cell-cell and cell-matrix interactions [5, 12].

ECM adhesion and assembly has a profound influence on cells. Besides providing a substrate for cell anchorage, it also guides the migration of cells during embryonic development and the wound repair process. ECM can play important roles in the differentiation of tissues. It is capable of transmitting environmental signals to cells, which affect various aspects of a cell's lifecycle like its proliferation, differentiation and death. Therefore, selection of an appropriate matrix for culturing cells is vital, as it can markedly affect the cellular responses [13].

The cellular microenvironment is recognised to be co-related to renal function. Renal disease progresses when ECM re-modelling occurs contributing to fibrotic scar tissue formation [14]. Excessive production of extracellular matrix components in conjunction with persistent kidney inflammation aggravates formation of fibrosis [15].

2.2. Kidney Disease

2.2.1. Chronic kidney disease (CKD)

Chronic kidney disease is a gradual loss of function and structural integrity of renal cells over a period of time. In 2007 CKD accounted for approximately 10 % of all deaths in Australia. The mortality rate due to CKD is rising alarmingly [2]. CKD often has no symptoms and is usually detected in the later stages of the disease [16]. As the disease progresses, viable nephrons are lost and when a substantial portion of the kidney tissue gets destroyed, the glomerular filtration rate starts declining [17]. As low molecular mass compounds start accumulating in the blood, uraemia occurs. Irrespective of the nature of the initial insult, in the early phases of the disease there is an interstitial infiltration of inflammatory cells that leads to induction of tubular injury. In the end state of CKD, fibrotic tissue replaces the viable nephrons in the kidney [9], leading to end stage renal disease (ESRD), cardiovascular diseases (CVD) and premature death.

Using conventional 2D cultures, studies performed in the Conjoint Renal Medicine Laboratory have successfully shown that PTEC of kidneys have immunomodulatory functions and can inhibit autologous immune responses under diseased inflammatory conditions. Activated primary PTEC under conditions mimicking inflammation can significantly decrease the proliferative responses of autologous T cells and also alter cytokine profiles [3]. This suggests that at earlier stages of the disease, when the kidneys are not yet substantially damaged, PTEC can play a very critical role in reducing the

inflammation and extent of damage to kidneys and limit progression to CKD [3]. Nonetheless, the 2D nature of these cell culture experiments does not match the native 3D environment of kidney. Therefore, this thesis aimed to investigate the immunomodulatory functions of activated primary human PTEC exerted on $CD4^+$ T cells under autologous settings in a more *in vivo* like 3D environment.

2.2.2. Mechanisms of kidney disease progression

The original hypothesis with respect to mechanisms of kidney disease progression focused on damage to the glomerular compartment of the kidneys. Observations and analysis by Ridson in 1968 on renal biopsy specimens from patients with persistent glomerular nephritis led them to hypothesise that progression of CKD is caused by an insult to the tubular interstitium instead [18]. Later, Cameron *et al.* demonstrated that there was significant correlation between ammonia concentration in urine and the degree of tubular atrophy and interstitial fibrosis which supported Ridson's speculations [19]. In contrast, some studies again insisted that kidney disease was glomerulocentric as they were able to show that changes in glomerular pressure in murine models contributed to injuries to the glomeruli both structurally and functionally [e.g. 20]. However, further studies involving both human and rat models established that damage or lesions in the renal tubular interstitium were of major importance in determining progressive damage to kidneys [21, 22]. Changes in the tubular interstitium of diabetic kidneys has also been shown to be related with a decrease in glomerular filtration rate and therefore kidney function [23]. Regardless of the disease aetiology it is now known that PTEC both respond and contribute to the disease process through a range of mechanisms.

2.2.3. Immunomodulatory role of PTEC

A pro-inflammatory environment is created within the kidney interstitium during the disease state. In response to injurious stimuli like high glucose, high protein levels and also diseases that cause inflammation in the kidneys, PTEC secrete waves of chemokines such as transforming growth factor beta (TGF-β) , regulated upon activation normal T-cell expressed and secreted (RANTES) [24], monocyte chemotactic protein-1 (MCP-1) [25] and interleukin-8 (IL-8) [26]. These result in extravasations of lymphocytes, monocytes and macrophages to the renal interstitium from the surrounding blood capillaries, which then secrete a secondary wave of cytokines including tumour necrosis factor-α (TNF-α), gamma-interferon (IFN-γ) and alpha-interferon (IFN-α) accentuating the inflammation (**Figure 2.2**). These inflammatory cytokines induce PTEC to up-regulate surface antigens, which include

major histocompatibility class I and II (MHC-I and II) [27], cluster of differentiation 40 (CD40) [28], inducible T-cell co-stimulator ligand (ICOS-L) [29] and inhibitory programmed death ligand-1 (PD-L1) [30]. The up-regulation of these surface antigens allows PTEC to act as non professional antigen presenting cells (APCs) and modulate immune responses [31].

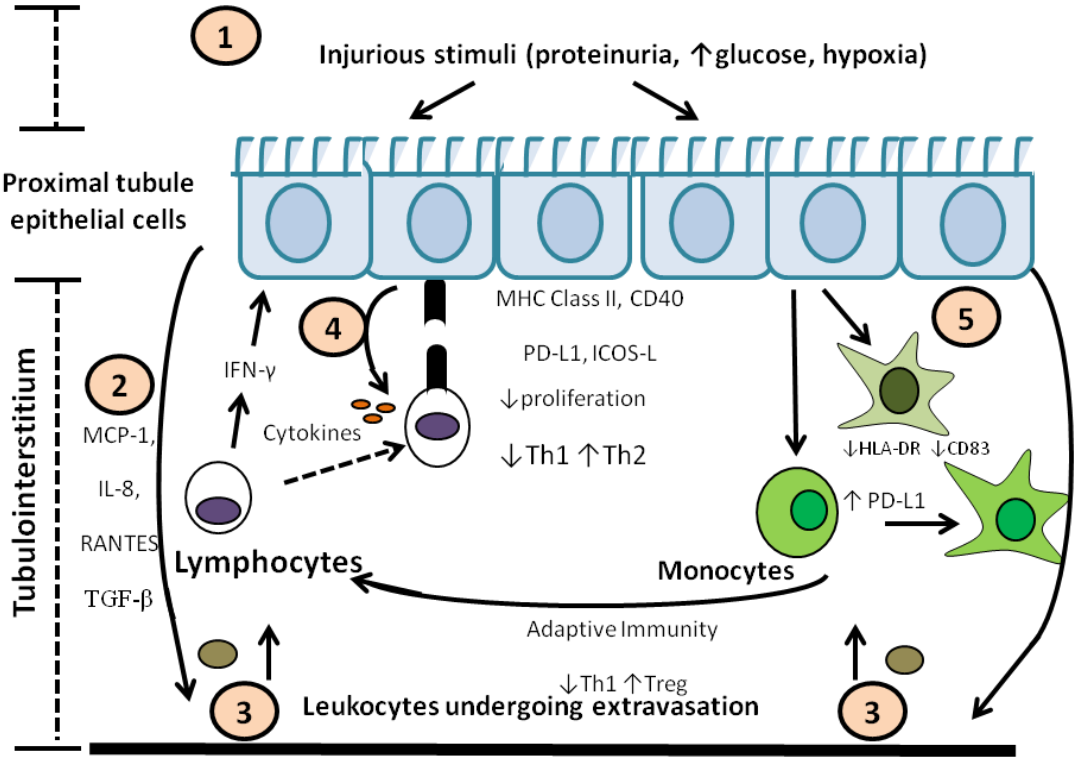

Figure 2.2 Schematic showing how PTEC in a perturbed disease state recruit lymphocytes into kidney interstitium and modulate functions of these cells.

(1) In the presence of injurious stimuli, the PTEC release (2) a range of chemokines e.g. MCP-1, IL-8 etc. (3) which aid in the recruitment of leukocytes from the surrounding blood capillaries. (4)These lymphocytes then release cytokines which help in up-regulation of cell surface markers on the PTEC (e.g. PD-L1). Interactions between the lymphocytes and PTEC subsequently lead to a decrease in proliferation of the immune cells accompanied by a cytokine shift away from an inflammatory Th1 effector profile to a Th2 type profile. (5) The PTEC also modulate dendritic cell function via complex interactions inducing weak Th1 responses (adapted from Healy *et al.* NHMRC grant application

MHC class II are a family of molecules that are constitutively expressed on professional APC, but may also be induced on other cells by IFN-γ [32]. MHC class II

molecules present antigen to $CD4^+$ T cells initiating the first signal for T cell activation. T cells require a second signal which may be a co-stimulatory or co-inhibitory one and this second signal determines whether the T cell undergoes activation or becomes unresponsive. This second signal is generated when the second receptor at the interface between APC and T cell binds [33]. If stimulated by IFN-γ, PTEC are capable of expressing MHC class II molecules thereby demonstrating ability to modulate $CD4^+$ T cell responses [34]. Our laboratory has also demonstrated that under inflammatory settings, PTEC up-regulate MHC Class II on their surface and modulate autologous human T cell responses [3].

In vitro studies confirmed that PD-L1 is expressed at low levels on normal human PTEC but is up-regulated significantly in response to inflammatory cytokines, particularly IFN-γ [3, 35, 36]. The promoter region of PD-L1 contains several IFN-γ responsive elements and hence under inflammatory conditions in the presence of pro-inflammatory cytokine IFN-γ, PD-L1 expression is up-regulated predominantly on non lymphoid tissues [37, 38]. PD-L1 interacts with PD-1 (CD279) receptor found on T cells causing decreased T Cell Receptor (TCR) mediated proliferation and cytokine production [39].

Thus it is likely that PTEC are capable of interacting with infiltrating immune cells in this perturbed inflammatory disease state. This has stimulated research using mouse models and allogeneic human systems [40, 41]. In an allogeneic model, transformed cell lines such as Human Kidney-2 (HK-2) cells, or primary PTEC from one donor are assayed against immune cells from a different donor. Results showed that PTEC are able to act as non-professional APC by expressing MHC-II, CD40, PD-L1 and ICOS-L antigens on their surface. Additionally, the expression of PD-L1 on PTEC may have a tissue protective function against cytotoxic $CD8^+$ T cell activity [42]. Further, renal expression of PD-L1 on human PTEC exerts an inhibitory effect on T cell responses [35, 43] and using αPD-L1 to block the ligand, it has been shown that PTEC were able to modulate T cell responses with respect to IL-2 secretion and CD69 expression [44].

Our laboratory, using 2D cell culture systems, has previously demonstrated that PTEC can modulate immune responses within the autologous human system. Results showed that primary human PTEC activated by treating with IFN-γ, down-regulate autologous T cells and that this down regulation is only partially mediated by PDL-1. This modulation was not caused by a decrease in activation markers or an increase in T- regulatory cells (T_{regs}) but by significant switching of cytokine profiles from T-helper type 1 (Th1) profile towards T helper type 2 (Th2) profile. Therefore, a significant decrease in IFN-γ, IL-2, TNF-α and increase in IL-4 production was seen [3].

In a more recently published paper, our laboratory has also demonstrated that in 2D cultures, human PTEC modulate autologous DC functions via complex interactions [45]. As the past observations have only ascribed a partial role to PD-L1 in down modulation of T cell responses, other immune-inhibitory molecules produced by PTEC were also examined in this thesis. One such molecule is the intracellular enzyme indoleamine 2, 3-dioxygenase (IDO). IDO is a tryptophan–catabolising enzyme and has immune suppressive effects on T cell functions [46].

Tryptophan is an essential amino acid that is required by T cells during proliferation. It is broken down to kynurenine during metabolism by the immunosuppressive enzyme IDO. IDO catalyses an initial step in the degradation of tryptophan along the kynurenine pathway thereby its presence limits the availability of tryptophan in the cellular microenvironment for T cell proliferation. The addition of 1 methyl-D-tryptophan (1MT) - an inhibitor of IDO in culture, allows tryptophan to be available to cells [47]. Earlier works on IDO suggested that cells that express IDO in an *in vivo* environment may act as APCs that can limit access to tryptophan during T cell activation [48]

The immunomodulatory role of IDO was initially discovered by Munn *et al*. They demonstrated that during pregnancy, IDO played a role in restricting T cell mediated rejection of the allogeneic foetuses [49]. Their work triggered further studies on the immunomodulatory potential of IDO and numerous studies have since identified the expression of this enzyme in various tissues and cells that includes placenta [50], brain [51, 52], liver [53], spleen [54], fibroblasts[55], endothelial cells [56], human bone marrow stromal cells [57] and many tumour cells [58, 59]. Myeloid cells such as DC and macrophages also produce IDO and are also able to inhibit T cell proliferation [60, 61]. This expression of IDO is regulated at the level of transcription. The gene for IDO has been cloned and shown to be differentially modulated by IFN-γ [62]. In response to IFN-γ and inflammatory stimuli, IDO expression is enhanced because the IDO promoter contains multiple promoter sequence elements such as interferon-stimulated response element (ISRE) and interferon-gamma activated sequence (GAS). Under inflammatory signalling, IDO induction occurs by phosphorylation of the latent signal transducer, activator of transcription 1 α (Stat1α) at the IFN-γ-receptor (IFNGR). Stat1 then forms a dimer and translocates to the nucleus where it binds gamma-activated sequences (GAS) to activate gene expression of IDO [63].

IDO expression has also been detected in mice kidney cells [64]. In mice, renal tubular epithelial cells express IDO when exposed to IFN-γ/TNF-α and promote apoptosis of tubular cells [65]. Some studies have demonstrated a correlation between IDO expression and CKD.

One study demonstrated that CKD patients having significantly elevated tryptophan metabolites in their serum compared to control groups [66].

2.2.4. T cell and their interactions with PTEC in kidney

2.2.4.1. T cell function

T lymphocytes or T cells are important cellular components of the immune system that play a critical role in cell-mediated immunity. The development of T cells occurs in the thymus and therefore their name is derived from it [67].

The primary function of T cells is to recognise non-self antigens or peptides bound to MHC molecules during antigen presentation and mount an appropriate immune response to eliminate the pathogen or infected cell. The recognition of a peptide-MHC complex occurs through a T cell antigen receptor (TCR) and acts as the first signal in the T cell activation process. Full T cell activation usually requires two further signalling events, (i) co-stimulation and (ii) cytokine exposure, both of which are provided by the APC [68].

There are different types of T cells and each type has a distinct function. The different classes include T helper cells (Th cells), Cytotoxic T cells (TC cells, or CTLs), Regulatory T cells (T_{reg} cells), Memory T cells and Natural Killer T cells (NKT). The two main classes of T cells are cytotoxic T cells and helper T cells. Cytotoxic or $CD8^+$ T cells recognise peptides presented by MHC Class I molecules and kill virally infected cells and tumours and also participate in organ rejection process.

Helper T cells, also known as $CD4^+$ T cells because they express the CD4 glycoprotein on their surface, recognise peptide antigens (Ags) presented by MHC Class II molecules and help activate macrophages, B cells, and cytotoxic T cells. When activated, helper T cells secrete a variety of signal proteins called cytokines that aid the immune response. These cells can be differentiated into one of several subtypes, including Th1, Th2, Th17, Th9, T_{regs} and follicular B helper T cells (T_{FH}), which secrete different cytokines to facilitate different types of immune responses. The differentiation is completely dependent upon the production of cytokines by APC. T cells are capable of migrating to distant sites and are believed to patrol almost all organs of the body, including the kidneys [69].

2.2.4.2. T cell interactions with PTEC in kidney

Many studies have suggested that T cells might play an important role during progressive loss of renal function [61, 62]. A study has reported that T cells isolated from renal biopsies can be grown *in vitro* and are able to specifically lyse PTEC in a cytotoxicity

assay [63]. Interestingly, under conditions that mimic renal diseases, PTEC secrete a wave of chemokines that causes T cells to infiltrate the kidneys and accumulate at the site of inflammation. PTEC also up-regulate a range of surface antigens that enable them to both modulate immune responses and become targets of cytotoxic T cells. Early studies with murine models have suggested that $CD4^+$ T cells infiltrate the kidney under inflammatory settings and activated PTEC can induce anergy in these infiltrating $CD4^+$ T cells [70]. Using allogeneic models, it has been demonstrated that under proteinuric conditions, human PTEC are also able to interact with T cells that infiltrate the kidney [25]. It has also been shown that in kidney diseases like chronic proteinuric nephropathy and chronic glomerulonephritis, T cells and PTEC interactions are regulated by the production of differential chemokines and chemokine receptors. Infiltrating T cells may interact with PTEC either via secreting soluble factors or by direct cell-to-cell contact [71, 72].

PD-1 is a transmembrane receptor of the immunoglobulin superfamily and has been shown to be expressed on thymocytes, mature T and B cells following activation and on myeloid cells [73]. In chronic infections or tumour invasion, the PD-L1/PD-1 pathway could be a key mechanism causing T cell exhaustion [39]. A study has previously demonstrated that in mouse, PTEC can act as APC to activate $CD4^+$ T cells whereby PD-L1 is able to modulate the T cell response by modulating expression of CD69 and production of IL-2 [44]. This study was translated into human studies by a Dutch group using an anti-CD3/CD28 T cell activation model to show that PTEC modulated T cell responses via PD-L1 and ICOS-L [41]. Further studies were carried out to confirm that PD-L1 expressed on PTEC surface can suppress alloreactive human T cell responses [43].

Our laboratory, employing 2D cultures, has previously demonstrated that the inhibition of autologous T cell responses by activated PTEC is partially mediated by the PD-L1/PD-1 pathway [3].

2.2.5. Chemokines and cytokines in kidney disease

Chemokines are a family of small, chemotactic cytokines that can attract leukocytes to sites of tissue damage or inflammation [74]. The human chemokine family is comprised of more than 40 ligands (L) and 19 corresponding receptors. The four subfamilies are categorised based on the number and spacing of the first two conserved cysteine residues in the amino terminus - CCL, CXCL, CX3CL1 and XCL1 [75]. The majority of the chemokines can bind to multiple chemokine receptors of the same subgroup and are also capable of acting as antagonists for chemokine receptors of other groups [76]. Functionally, chemokines can be grouped into ‘inflammatory’ chemokines that are inducible and

'homeostatic' chemokines that are constitutively expressed by cells. Inflammatory chemokines attract effector leukocytes to sites of inflammation by causing extravasations through the blood vessels. The leukocytes then migrate along the chemokine gradient to reach the source. These inflammatory cells can release cytokines and growth factors to intensify the response and promote further injury. Growing evidence suggests that in kidney diseases, the influx of T cells and macrophages/monocytes into kidneys play a pivotal role in promoting interstitial fibrosis and the progression of CKD [77]. Research in renal diseases has mostly been focused on the inflammatory chemokines [78, 79].

Expression of chemokines in renal diseases has been reported to be correlated with the accumulation of effector leukocytes and renal damage. Animal models have been studied to characterise expression of chemokines in various kidney diseases and relevance has been established for expression of chemokines in human diseases by investigating human renal biopsies [77, 80]. Research on human PTEC has shown that in the presence of proinflammatory cytokines, PTEC produces significant amounts of RANTES/ CCL5 (by TNF-α and IFN-γ) [24], interferon gamma-induced protein 10 (IP-10)/ CXCL10 (by IFN-γ and TNF-α) [25], MCP-1/CCL2 (by TNF-α and IFN-γ) [71], IL-8/CXCL8 (by TNF-α) and fractalkine/CX3CL1 (by TNF-α) [81]. These chemokines can attract T cells expressing the receptors CCR5, CX3CR1 [82] and significantly a greater number of $CD4^+$ T cells expressing CXCR3 [83]. All these findings were made using cell lines or 2D allogeneic cell culture models. The expression patterns of chemokines from human PTEC in an *in vivo*-like 3D environment has not been yet reported.

Using 2D cultures, our laboratory has also studied expression of cell surface molecules up-regulated by PTEC under the influence of different proinflammatory cytokines which included IFN-α, IFN-γ, TGF-β and TNF-α. Amongst these inflammatory cytokines, only IFN-γ seemed to have a major effect on the up-regulation of PD-L1 and MHC class II expression on PTEC. When IFN-γ and TGF-β were used in combination, an additive effect on the expression of PD-L1 on PTEC was observed [3].

This thesis focused on the expression patterns of cell surface molecules on PTEC under the influence of proinflammatory cytokines in 3D cultures, and also on the expression patterns of chemokines in 2D and 3D *in vitro* models under the influence of proinflammatory cytokines.

2.3. Tissue engineering and cell culture models

2.3.1. 2D cell culture models

Cell culture in two dimensions (monolayer) is commonly used in most laboratories, but does not closely approximate the *in vivo* environment of cells.

In vivo, PTEC line the proximal tubule attached to a basement membrane on their basolateral side, where they can interact with immune cells within a 3D environment. Nonetheless, most of the experimental studies with PTEC commonly employ 2D culture systems to investigate individual cell types and interactions, which may have its limitations. At the very least, such cultures would see responding cells interacting with the apical side of the cultured PTEC instead of the basolateral side, as would occur *in vivo*. While it is relatively straightforward to use these cell culture models, 2D cultures and co-cultures do not always reflect the cellular responses seen in their *in vivo* analogues [82, 84, 85] and it seems logical to assume that the introduction of a 3D culture system would provide more relevant biological data and new insights. Study of cell migration using a 3D cell culture model and *in vivo* has revealed several differences when compared with cell migration in 2D, including cell morphology and mechanical and signalling control [86].

2.3.2. 3D cell culture models

Organ culture is among one of the oldest 3D culture techniques [87]. Although organ culture can resemble and provide information of *in vivo* events, but maintaining a direct organ culture is exceptionally difficult. The limiting factors include inability to precisely control different variables like oxygen diffusion to inner cells of the organ leading to high cell mortality. Organoid kidney 3D cultures have also been developed by encapsulating intact proximal tubule fragments in a hydrogel [88]. This model design retained cell-cell, cell-matrix, and tissue architecture and had been used for screening drug toxicity. But the major drawbacks of these cultures are the technical complexities, the meticulous and laborious preparations of the constructs, and insufficient oxygen diffusion into the deepest layers in the complex 3D model [88, 89].

Hydrogels are the most prevalent and versatile 3D models for *in vitro* studies; these provide a well-hydrated matrix with options for tailoring matrix stiffness, cell adhesivity and degradability [6]. These are very promising when it comes to biomedical applications and are being used as drug and cell carriers, tissue engineering matrices, among others. Major

advantages of hydrogel systems are their similarities with natural tissues and their biocompatibility [90]. Hydrogels can also be tailored with specific biological features such as basement membrane components [91]. Additionally, these can be used to study specific cell interactions in a more controlled setting which is less complex than organ culture. Several types of hydrogels may be useful in the study of PTEC-immune cell interactions, ranging from simple and inert (such as alginate), to complex and highly cell active (such as Matrigel).

Alginate hydrogel has structural similarity to extracellular matrices in tissues and has been extensively investigated and used for many biomedical applications [92]. Alginate is a naturally occurring polysaccharide typically extracted from brown algae (Phaeophyceae). It consists of a family of linear copolymers containing blocks of (1, 4)-linked β-D-mannuronate (M) and α -L- guluronate (G) residues. The blocks are composed of consecutive G residues consecutive M residues and alternating M and G residues. Alginate can undergo ionic cross-linking where only G blocks are believed to take part in intermolecular cross-linking with divalent cations (e.g., Ca^{2+}, Mg^{2+}) to form hydrogels. This process is reversible through addition of chelating agents, such as ethylene diamine tetra-acetic acid (EDTA), thus allowing easy dissolution of the gels. Alginate is most frequently cross-linked ionically with calcium chloride ($CaCl_2$) solution in a gelation process that relies on the diffusion of Ca^{2+} ions into the alginate and often results in inhomogeneous gelation due to ion gradients within the gel. An alternative method for cross-linking alginate gels has been described by Kuo and Ma [93]. In this method calcium carbonate ($CaCO_3$) is used as a source of calcium ions together with D-(+)-gluconic acid δ lactone (GDL) to initiate the process of gelation in the sodium alginate solution. This way a slower gelation rate is achieved by the slow release of calcium from the insoluble $CaCO_3$, producing gels that are more uniform in structure and porosity. Uniform porosity ensures nutrients are able to diffuse through the gel to reach cells in the centre [94]. While alginate allows for straightforward encapsulation and recovery of cells, it lacks cell adhesion sites and allows no interaction between the gel and the cells [92]. Therefore, additional components may be required to model an interactive cell-extracellular matrix environment.

Collagens, predominantly type I, are the main protein component of connective tissues in mammals, and thus are a good candidate for interactive components in a 3D culture system [95]. Collagens are high in glycine, representing every third position in the amino acid chain (gly-X-Y), and are responsible for the helical structure of collagen [96]. Acidic solutions of collagen can be adjusted for physiological pH at low temperatures (less than 10 ˚C) and warmed to a higher temperature of 37 ˚C for about an hour to form a translucent gel [97]. These gels undergo dissolution if treated with collagenase enzymes. 3D gels of

collagen fibres have been used in the early 1980s by Schor *et al*. to study the migration and cell behaviour of different cell types *in vitro* [98-100]. Lymphocytes are highly motile cells constantly circulating in the blood, which under certain conditions undergo extravasations to migrate into the perivascular tissue space [101]. Collagen fibres are believed to be one of the main components of the tissue stroma through which lymphocytes migrate *in vivo* [102]. However, the complete understanding of the mechanism of T lymphocyte migration with respect to interactions with the extracellular matrix components is yet to be unveiled. Some groups of researchers have studied the roles of various components of the extracellular matrix using collagen as the 3D matrix to understand how these affect T cell invasion into tissues [103-105]. In the early 1990s, a study by the Sundqvist group showed that T cells migrate through 3D collagen substrata by adhesive mechanisms [106]. The Madin-Darby Canine Kidney (MDCK) cell line has also been cultured and studied in collagen gels [107]. A study with MDCK reported significant differences in cell behaviour when cultured in 2D and 3D [108]. Primary human PTEC isolated from urine were grown between two layers of collagen to successfully form three-dimensional structures [109]. Therefore, collagen comprising of natural proteins may be used in combination with alginate to provide cell adhesion sites for these cells in the gel.

Gelatin-methacrylamide (GelMA) is a photocrosslinkable hydrogel that is derived from inexpensive gelatin. Gelatin is water soluble and made by denaturing collagen [110]. Gelatin has a wide use in tissue engineering applications, particularly for 3D cell culture models due to its biocompatibility, biodegradability, and ability to form hydrogels [111, 112]. Unsaturated methacrylamide groups can be added to the amine containing side groups of gelatin under mild conditions to make a photo-polymerizable hydrogel that is stable at 37 ˚C [113]. Different cell types including immortalized human umbilical vein endothelial cells (HUVEC), NIH 3T3 fibroblasts [110] and aortic valvular interstitial cells (VIC) [114] have been encapsulated and cultured within GelMA gels. Our collaborating laboratory at IHBI, QUT has successfully shown that chondrocytes have a high cell viability within GelMA hydrogel and is a good candidate for cartilage tissue engineering [115]. This thesis intends to test the suitability of GelMA as a potential matrix for the co-culture of autologous PTEC and immune cells.

While collagen-based hydrogels provide cell adhesion sites and other protein motifs, they are limited to a single protein, and therefore may not represent the native extracellular microenvironment very well. Thus, there is benefit in exploring models based on more complex protein/proteoglycan mixtures. Matrigel is an extract containing basement membrane proteins and growth factors derived from Engelbreth-Holm-Swarm (EHS) mouse sarcoma [116]. It forms a 3D gel around physiological temperatures and also promotes

differentiation and proliferation of many different cell types [91]. Matrigel is a complex mix of proteins and abundant in basement membrane proteins like laminins, type IV collagen, perlecan and nidogen/entactin. It also contains growth factors, such as transforming growth factor β (TGF-β), fibroblast growth factor (FGF), epidermal growth factor (EGF), platelet derived growth factor (PDGF) and insulin-like growth factor (IGF) [91, 117].

Matrigel could be a good candidate for serving as a 3D matrix for PTEC as research has shown that renal PTEC have a high cell attachment and proliferation on Matrigel [118]. To keep the influence of growth factors as low as possible growth factor reduced (GFR) Matrigel will be used. However, the handling of Matrigel hydrogels is challenging as these gels are very soft and easily disintegrate during culture. Therefore, combining Matrigel with alginate is a promising approach, as the addition of alginate could increase the stability and stiffness of Matrigel hydrogels while maintaining their biological activity.

Combinations of gels with varying matrix properties have already been used for the co-culture of different types of cells [119]. However, recovering these cells from the matrix to further dissect the mechanisms of interactions between them is not very common.

Attempts to engineer 3D *in vitro* models for normal and diseased kidney have been made by co-culturing immortalized mouse embryonic kidney (MEK) epithelial cells with mouse fibroblasts within silk-based porous scaffolds with collagen-matrigel content [120]. Most recently to build a human *in vitro* model that mimics the renal proximal tubule, small intestinal submucosa (SIS) was used as a scaffold to grow cadaveric human kidney-derived cells (hKDc) [121].

2.4. Hypotheses

In view of the current literature, it was proposed that there were no evidences of how 3D *in vivo* like environment influenced co-culture of primary human PTEC and autologous immune cells.

Therefore the aim was to fill this gap of knowledge by investigating the influence of a more physiologically relevant 3D model on the interaction of these two types of cells. We proposed to define a 3D *in vitro* model that could sustain both the kidney PTEC and immune cells. We hypothesized that studying these two types of cells within a 3D environment would provide new and interesting insights into their interactions. The results obtained from the 3D culture were compared with studies carried out using the conventional 2D culture system.

2.5. Aims

1. Define a suitable hydrogel capable of maintaining viability and function of purified T cells and autologous PTEC within the hydrogel.
2. Develop techniques for recovery of the immune cells and the PTEC from the hydrogel for analysis.
3. Monitor the immunomodulatory function of PTEC in the defined model system.

Chapter 3: Materials and Methods

This chapter contains an overview of the materials and methods used throughout the thesis.

3.1. Materials

Table 1: Materials used

REAGENTS	FINAL CONCENTRATION	SUPPLIER
DMEM F12		Invitrogen; Catalogue No.: 11330057
Fungizone		Invitrogen ; Catalogue No.: 15290018
Sterile Scalpel		Swann-Morten Disposable Sterile Scalpels Ref No. 0508
100 µm Nylon Cell Strainer		BD Falcon; Catalogue No.: 352360
40 µm Nylon Cell Strainer		BD Falcon; Catalogue No.: 352340
HEPES Buffer		Invitrogen; Catalogue No.: 15630-08
L-Glutamine and Pyridoxine Hydrochloride		Invitrogen
Epidermal Growth Factor	10 ng/mL	Sigma-Aldrich; Catalogue No.: E9644
Hydrocortisone	36 ng/mL	Sigma-Aldrich; Catalogue No.: H0396

Tri-Iodothyronine	4 pg/mL	Sigma-Aldrich Catalogue No.: T5516
Penicillin-Streptomycin	Penicillin 100 U/mL Streptomycin 100µg/mL	Invitrogen Catalogue No.:15140-122
ITS (Insulin –Transferrin-Selenium)	Insulin 10µg/mL Transferrin 5µg/mL Selenium 5ng/mL	Sigma-Aldrich; Catalogue No.: I1884-1VL
TrypLE™ Express		Invitrogen; Catalogue No.: 12604-021
TrypLE Inhibitor		Invitrogen; Catalogue No.: R007-100
IFN-γ	100 ng/mL	R&D Systems; Catalogue No.: 285-IF-100
IL-4	1000 U/mL	Miltenyi Biotech Catalogue No.: 130-093-922
Ficoll		GE Health; Catalogue No.: 17-1440-03
Sterile Syringe		Terumo syringes Luer lock 50mL Catalogue no.1260603
Sterile Cannula		Uno medical Catalogue No. 500.11.012
Haemocytometer		Boeco
Trypan Blue		Sigma
Olympus Cx40		Olympus Corporation
^{3}[H]-Thymidine	5 µCi/mL	Perkin Elmer
90 X 120 Mm Glass Fibre Filter Mat		Perkin Elmer
90 X 120 Mm Filter Mat Sample Bags		Perkin Elmer
Human CD4 Micro-Beads		Miltenyi Biotech; Cat No.: 130-045-101

Anti-PD-L1	10 µg/mL	Bio Legend Catalogue No.: 329702
Phytohaemagglutinin (PHA-P)	10 µg/mL	Sigma-Aldrich; Catalogue No.: L8754-5MG
Anti Human CD3	0.5 µg/mL	Abcam Catalogue No: AB8090
Anti Human CD28	0.1 µg/mL	Abcam Catalogue No.: AB85986
Collagenase P	1 mg/mL	Roche Catalogue No.: 11 213 857 001
Collagenase From *Clostridium Histolyticum*	1 mg/mL	Sigma-Aldrich Catalogue No.: C6885-1g
DNase I	20µg/mL	Roche Catalogue No.: 11284932001
Carboxyfluorescein Diacetate Succinimidyl Ester (CFSE)	0.5µm	BioLegend
Labtek 11 Chambered Cover Glass Non Removable Upper Chamber		Thermo Fisher Scientific Catalogue No.: NUN155409
0.2µ filter		Minisart Sartorius Catalogue No.:16534k
Bovine Serum Albumin (BSA)		Sigma-Aldrich Catalogue No. :A7906-100G
DAPI	5 µg/mL	Sigma-Aldrich Catalogue No. :D9542-5MG
Rhodamine Phalloidin	0.8U/mL	Invitrogen Catalogue No. : R415
16% Paraformaldehyde (PFA) methanol free		Electron Microscopy Sciences Catalogue No. :15710
Collagen Solution		Sigma-Aldrich Catalogue No. :C4243
Gelatin methacrylamide (GelMA)		Obtained from CRL, IHBI, QUT.

Fluorescein diacetate (FDA)	10 μg/mL	Invitrogen Catalogue No. : F1303
Propidium Iodide (PI)	5 μg/mL	Invitrogen Catalogue No. : P21493
Monoclonal rabbit IgG anti-human E-Cadherin	1 in 150 dilution	Cell Signalling Technology Catalogue No. : 3195 clone 24E10
Alexa Fluor® 647 – labelled lectin PNA from *Arachis hypogaea* (peanut)	20μg/mL	Invitrogen Catalogue No. : R415
Mouse anti-human collagen type IV (IgG1κ)	3.5μg/mL	DSHB, USA Clone M3F7
Alexa Fluor® 488 – labelled Affinipure donkey anti-mouse IgG (H+L)	4.7 μg/mL	Jackson ImmunoResearch Catalogue No. :115-585-152
Alexa Fluor® 594 – labelled Affinipure donkey anti-rabbit IgG (H+L)	4.7 μg/mL	Jackson ImmunoResearch Catalogue No. : 711-585-152
Alginate powder		Pronova UP LVG, Novomatrix Catalogue No. :4200006
Matrigel™ matrix		BD Biosciences Catalogue No. : 356231
Irgacure 2959 (2-hydroxy-1-[4-(2-hydroxyethoxy)phenyl]-2-methyl-1-propanone)	2.5 mg/mL	BASF, Ludwigshafen, Germany
24w Plate, Ps, TC Treated, F-Bottom, W/ Lid		Greiner Bio-One Catalogue No.: 662160
Dulbecco's Phosphate Buffered Saline ,Ca And Mg Free (PBS)		Invitrogen Catalogue No. :14190-144

BD Cytometric Bead Array (CBA) Human Chemokine Kit		BD Biosciences Catalogue No. : 552990
BD Cytometric Bead Array (CBA) Human Th1/Th2 Cytokine Kit II		BD Biosciences Catalogue No. : 551809
BD Cytometric Bead Array (CBA) Human Inflammatory Cytokines Kit		BD Biosciences Catalogue No. : 551811
D-(+)-Gluconic acid δ lactone (GDL)	60mM	Sigma-Aldrich Catalogue No. G4750-100G
TNF-α	20ng/mL	R&D Systems (from Bioscientific) Catalogue No. 210-TA-020
1-Methyl-DL-Tryptophan (1MT)	1500µM/mL	Sigma-Aldrich Catalogue No. 860646
Transforming growth factor -1 (TGF-β 1)	20 ng/mL	R & D systems.

3.2. Cell culture

3.2.1. Origin of PTEC

Following ethics approval and informed consent, kidney tissue was obtained from the healthy portion of tumour nephrectomies. Cortex tissue was dissected from macroscopically/microscopically normal portions of the kidney and processed for PTEC purification within 1 h.

PTEC were purified following the method of Glynne and Evans [122] and cultured in defined medium (DM) comprised of 1:1 mixture of Dulbecco's modified Eagle's medium (DMEM) and Ham's F12 containing 15 mM HEPES buffer, L-glutamine and pyridoxine hydrochloride. The medium was supplemented with epidermal growth factor (10 ng/mL), insulin (10 µg/mL), transferrin (5 µg/mL), selenium (5 ng/mL), hydrocortisone (36 ng/mL), tri-iodothyronine (4 pg/mL), penicillin (100 U/mL), streptomycin (100 µg/mL). Briefly, the cortex of the kidney was detached from its outer capsule, washed thoroughly using DMEM media supplemented with fungizone and cut into small pieces of an approximate size of 1 mm^2 using a sterile scalpel (Labtech). The tissue was then digested using collagenase (Sigma C6885, 1 mg/mL) for 1 hr at 37 °C with vortexing every 10 min. The resulting cell suspension was passed through a 100 µm nylon cell strainer (BD falcon) followed by a 40 µm nylon cell strainer (BD falcon). The flow-through was centrifuged at 1000 rpm for 5 min. The supernatant was discarded and the pellet was resuspended in DM.

Cell stocks were frozen at passage 1 (P1), and all PTEC were used in final experiments between P2 and P3. PTEC were characterized on the basis of (i) strong staining for cytokeratin-18, (ii) strong staining for alkaline phosphatase activity using the naphtal AS-MX method and (iii) characteristic cobblestone morphology.

3.2.2. Maintenance of PTEC

PTEC were cultured in DM at 37 °C with 5 % CO_2 under constant humidity.

3.2.3. Passage of PTEC

Where required, cells were passaged when they were 80 % confluent to maintain optimum viability. The supernatant was removed and the cells washed twice in Mg^{2+} and Ca^{2+}-free phosphate-buffered saline (PBS). TrypLE™ Express (1x) was added to the cell monolayer to detach the cells from the culture flask. Following incubation at 37 °C for 5 minutes, trypsinization of cells was stopped by adding an equal volume of Defined Trypsin inhibitor (Invitrogen). Cells were washed twice in DM and re-suspended at a 1 in 10 dilution for passaging.

3.2.4. Cryopreservation of PTEC

For PTEC cryopreservation, following centrifugation the cells were resuspended in a final concentration of $1x10^6$-$2x10^6$ cells/mL in serum-free cryopreservation media constituting of 90 % DM media and 10 % dimethyl sulfoxide (DMSO) (Sigma-Aldrich). 1 mL aliquots of cell suspension were then distributed into thermo scientific cryotube vials and placed in a -80 °C freezer in Mr. Frosty Cryo freezing containers (Nalgene). After 24-48 hours, cells were transferred to liquid nitrogen for long-term storage.

3.2.5. Revival of cryo-preserved PTEC

To thaw the PTEC, cells were quickly removed from liquid nitrogen and warmed to room temperature by transferring to a 37 °C water bath. To prevent osmotic lysis, culture media was added to the cell suspension very slowly drop-wise. The resulting cell suspension was centrifuged at 190 g for 5 minutes and the cell pellet re-suspended in DM before transferring to a cell culture flask. PTEC were maintained as described in section 3.2.2.

3.2.6. Activation of PTEC

P2 PTEC were cultured in DM until 70-80 % confluent and exposed to IFN-γ (100 ng/mL), for 36 hrs. Cells were gently detached with TrypLE™ Express (1x), neutralized immediately with Trypsin inhibitor (Invitrogen), washed once in DM and

re-suspended in DM for culture experiments or phosphate-buffered saline (PBS) containing 0.02 % sodium azide and 0.5 % bovine serum albumin (BSA) (FACS buffer) for cell staining .

3.2.7. Irradiation of PTEC

Where required, PTEC were exposed to γ-radiation at 30 Gy in a Gamma-cell irradiator to prevent further cell division.

3.2.8. Origin of Blood cells

Blood was obtained from the same donors 3 to 6 months post-nephrectomy. PBMC were isolated by Ficoll-density gradient separation (refer section 3.2.9). $CD4^+$ T cells were purified from PBMC using Miltenyi Microbeads (Sydney, Australia) following the manufacturer's instructions (refer section 3.2.12).

3.2.9. Peripheral blood mononuclear cells (PBMC) enrichment from whole blood

For PBMC isolation by Ficoll-density gradient separation, 20mL blood was diluted 1:2 with sterile room-temperature PBS in a 50 ml Falcon tube and underlain with 10 mL Ficoll-Paque™ Plus (GE Healthcare) using a sterile syringe fitted with a sterile cannula. Samples were centrifuged at room-temperature at 373 g for 20 min with brakes turned off. PBMC were then carefully collected from the Ficoll interface with a sterile plastic transfer pipette, washed 3 times in ice cold PBS, and resuspended in either complete medium (CM) consisting of Roswell Park Memorial Institute medium 1640 (RPMI-1640) supplemented with 2 mM glutamine, 10 mM HEPES (4-(2-hydroxyethyl)-1-piperazineethanesulfonic acid), 1 mM pyruvate, 0.1 mM nonessential amino acids, 50 µM 2-mercapto ethanol, penicillin (100 U/mL), streptomycin (100 µg/mL) and 10 % heat-inactivated human AB serum for use in subsequent experiments or put into freezer medium (50 % Fetal Calf Serum (FCS) 40 % RPMI-1640 medium,10 % dimethylsulfoxide (DMSO)) for cryopreservation (refer section 3.2.10).

3.2.10. Cryopreservation of PBMC

Appropriate volumes of cryopreservation media comprising of 10 % DMSO (Sigma-Aldrich), 50 % heat-inactivated foetal calf serum (FCS) and 40 % RPMI media were slowly added to PBMC for a final concentration of $25x10^6$ cells/mL. 1 mL aliquots of cell suspension were then distributed into thermo scientific cryotube vials and placed in -80°C freezer in Mr. Frosty Cryo freezing containers. After 24-48 hours, cells were transferred to liquid nitrogen for long-term storage.

3.2.11. Revival of cryo-preserved PBMC

Upon removal from liquid nitrogen, PBMC were transferred to a 37 °C water bath as fast as possible until completely thawed. Culture media was added to the cell suspension drop-wise very slowly in order to prevent osmotic lysis of the cells. The cell suspension was washed twice (centrifuged at 373 g for 5 minutes) and the cell pellet re-suspended in CM for use in experiments.

3.2.12. $CD4^+$ T cell isolations from PBMC

Following manufacturer's instructions, $CD4^+$ T cells were purified from PBMC using Miltenyi Microbeads (Sydney, Australia). Briefly, PBMC isolated from donor blood were counted and washed at 373 g for 5 minutes. Supernatant was completely removed and cells resuspended in 80 µL of MACS buffer comprising of 0.5 % BSA, 2 mM EDTA and Ca^{2+}/Mg^{2+}-free PBS per 10^7 total PBMC. 20 µL of CD4 microbeads (Miltenyi Biotech) were added per 10^7 cells. The cell suspension was incubated in the fridge for 15 minutes, with minor mixing every 5 minutes, followed by a wash at 373 g for 5 minutes. Supernatant was removed completely and cells re-suspended in 500 µL of MACS buffer/10^8 cells. The suspension was passed through a column (LS column Miltenyi Biotech) placed in a magnetic field. Unlabelled cells that passed through the column were collected as"flow-through". Following 3 x 500 µL washes, the column was removed from the magnetic field and a plunger was used to flush magnetically labelled $CD4^+$ T cells out of the column. Based upon CD4 staining, the purity of $CD4^+$ T cells was generally greater than 96 %.

3.2.13. Cell counting

A cell sample was diluted 1:2 with trypan blue (Sigma) and mixed thoroughly. 10 µL of cell suspension was then loaded into the haemocytometer counting chamber (Boeco, Germany). Live cells, marked by trypan blue exclusion, were counted from one or more corner squares of the haemocytometer counting area using an Olympus CX40 phase contrast microscope (Olympus Corporation). Cell concentration was calculated using the formula:

Cell concentration/mL = (Average number of live cells counted from one or more corner squares of the haemocytometer) X (dilution factor) X 10^4

For a viability count in a given sample, dead cells, stained blue with trypan blue, were also counted to obtain the total number of cells and percentage viability was calculated as:

Viability percentage = (Average number of live cells counted from one or more corner squares of the haemocytometer / Average number of all cells counted from one or more corner squares of the haemocytometer) X 100

3.3. Fabrication of hydrogels

To define hydrogel constructs for optimal interaction and viability of immune cells and PTEC in co-cultures, various combinations of different gels were studied.

3.3.1. Cell encapsulation and cell differentiation in different gel mixtures

3.3.1.1. Alginate gel preparation

A stock solution of 2 % (w/v) Alginate was prepared by dissolving alginate powder (Pronova UP LVG, Novomatrix) in normal saline (150 mM) and the mixture

filter sterilised. To achieve controlled gelation, sterile alginate solution was mixed with sonicated Calcium Carbonate ($CaCO_3$, 30 mM) suspension and kept at a temperature of 2-4 ˚C. Alginate solution had a final concentration of 1 % in the resulting gel mixture. $CD4^+$ T cells ($1x10^6$ cells/ml) and PTEC ($5x10^5$ cells/ml) were washed at 1400 rpm for 5 mins and re-suspended in the alginate-$CaCO_3$ suspension. Freshly prepared D-(+)-gluconic acid δ lactone (GDL, 60 mM) was added to alginate-$CaCO_3$ mix containing cells. The mixture was gently pipetted up and down to obtain a homogenous solution. The resulting mixture was put in glass slide chambers (Thermo- Fisher Scientific) in 50 µl droplets and incubated at 37˚C and 5 % CO_2 for approximately 30 mins until gel formation occurred. CM was added to the gels. The gels were incubated and viability of cells was checked at different time points (refer section 3.9).

3.3.1.2. Matrigel gel preparation

$CD4^+$ T cells ($1x10^6$ cells/ml) and PTEC ($5x10^5$ cells/ml) were washed and mixed gently with Matrigel™ matrix (0.9 % w/v, growth factor-reduced, phenol red free; BD Bioscience, Bedford, MA, USA). Cold sterile tips were used to add the Matrigel - cells mix into glass slide chambers (Thermo- Fisher Scientific) and incubated at 37 ˚C 5 % CO_2 for 25-30 mins until gels formed.

3.3.1.3. Alginate – Collagen gel preparation

Collagen type I solution (Sigma-Aldrich) was first neutralized and pH adjusted according to manufacturer's instructions. Briefly, 8 parts of chilled collagen solution was mixed with 1 part of sterile 10X PBS. The pH was adjusted to 7.2-7.5 by adding sterile 0.1 M NaOH. To prevent gelation of collagen, the temperature was maintained at 2-8 ˚C.

Alginate (Pronova UP LVG, Novomatrix) solution was prepared as described in section 3.3.1.1. To 50 µL of stock alginate solution, 5 µL of $CaCO_3$ and 40 µL of neutralized collagen solution were added. This suspension was mixed with cells. The final concentration of $CD4^+$ T cells was $1x10^6$ cells/ml and PTEC was $5x10^5$ cells/ml in the gel. Finally, 5 µL of freshly prepared GDL was added to this mixture before it was pipetted into glass slide chambers (Thermo- Fisher Scientific) in 50 µL droplets

and incubated at 37 ˚C in a humidified atmosphere of 5 % CO_2 for 30 mins until gels formed. CM was added to the gels for culture. Cells encapsulated within gels were analysed at different time points for cell viability (refer section 3.9).

3.3.1.4. Alginate- Matrigel construct preparation

A stock solution of alginate (Pronova UP LVG, Novomatrix) was prepared (refer section 3.3.1.1) and combined with Matrigel^{TM} matrix (0.9 % w/v, growth factor-reduced, phenol red free; BD Bioscience, Bedford, MA, USA). Briefly, 50 µL of 2 % alginate was mixed with 5 µL of $CaCO_3$ (300 mM) and 40 µL of Matrigel. To this mix, cells were resuspended keeping the final concentration of $CD4^+$ T cells $1x10^6$ cells/ml and PTEC $5x10^5$cells/ml. The mixture was gently pipetted up and down to obtain a homogenous suspension before being put into glass slide chambers (Thermo- Fisher Scientific) and incubated at 37 ˚C & 5 % CO_2. After 25-30 mins when the gels had formed, CM was added to the gels. Cell viability was analysed as described in section 3.9.

3.3.2. GelMA cell culture model

GelMA was generously supplied by the Cartilage Regeneration Laboratory (CRL) at IHBI, QUT. Briefly, Type A gelatin (Molecular weight [MW] ~ 90 kDa) purchased from Sigma-Aldrich was modified to include photocrosslinkable groups by reaction with methacrylic anhydride (MAAh) (Sigma-Aldrich). Gelatin was dissolved in PBS (Invitrogen, Carlsbad, CA) at 100 mg/mL and reacted with 0.6 g MAAh per gram gelatin for 1 h at 50 ˚C under continuous stirring. Insoluble MAAh was removed by centrifugation, and remaining MAAh was removed by dialysis against distilled water (12 kDa MWCO cellulose dialysis membrane, Sigma-Aldrich). Functionalized polymers were lyophilized.

A GelMA stock solution of 6.25 % (w/v) from the lyophilized GelMA (obtained from CRL, IHBI) was prepared a day in advance. First, preheated sterile PBS (70 ˚C) was added to photoinitiator (PI): 2-hydroxy-1-[4-(2-hydroxyethoxy) phenyl]-2-methyl-1-propanone (Irgacure 2959) to make a 2.5 mg/mL solution. The mix was then placed in 70 ˚C water bath and shaken until completely dissolved. Following filter sterilisation through a 0.2 µm filter (Minisart Sartorius), the PI was

diluted 4 times in sterile PBS. Appropriate amount of GelMA to make 6.25 % was measured and added to the diluted PI supplemented PBS. The tube was wrapped in foil and left overnight at 4 ˚C.

The next day soaked GelMA was warmed in a water bath (37 ˚C) until it completely dissolved. $CD4^+$ T cells (final concentration in gels $1x10^6$ cells/ml) were washed at 373 g for 5 minutes and resuspended in sterile PBS in 1/5 of the final volume of GelMA solution. Prepared PI supplemented GelMA solution was added to it and mixed well. Final concentration of GelMA was 5 % (v/v of stock solution) and PI was 0.5 mg/mL. The GelMA–cell mix was pipetted into Teflon moulds (Figure 3.1) slightly over filling the grooves to avoid air bubbles. Sterile microscopic glass slides were placed to cover the moulds and placed in the centre of a photo-cross linker (wavelength = 365 nm). After 5 minutes the gels were removed from the mould and cut into 10 x 5 mm gels using a cutting guide.

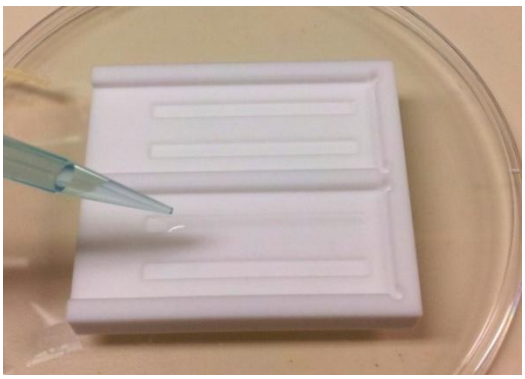

Figure 3.1 Teflon Mould for GelMA gels.

The gels were placed in a 24 well flat bottomed plate (Greiner Bio-one) and 1 mL of CM was added to the gels in each well. Incubation was continued for 1 hour at 37 ˚C in a humidified atmosphere of 5 % CO_2. After 1 hour the media was taken out and 5 µL of PTEC (concentration = $2X10^6$ cells/mL) was added on top of the gels. This was incubated for 3 hours under the same conditions. At the end of 3 hours when the PTEC had attached to the gel surface, warm CM was added and the gels incubated at 37 ˚C and 5 % CO_2. At different time points the gels were taken out of the cultures to monitor viability and stain for various cell surface and intracellular markers.

3.3.3. Type I Collagen gel culture model.

Collagen type I solution (Sigma-Aldrich) was first neutralized and pH adjusted according to manufacturer's instructions as described in section 3.3.1.3. Chilled neutral collagen was transferred to 96 well flat bottomed plates (Nalgen Nunc International) at 50 µL/well to coat the wells with an acellular layer of collagen. The mixture was allowed to polymerize for approximately 1 h at 37 ˚C. $CD4^+$ T cells were used at a concentration of $1x10^6$ cells/ml and PTEC at $1.5x10^5$ cells/ml for proliferation assays. For wells containing $CD4^+$ T cells in gels, 200 µL of the cell suspension was transferred to an Eppendorf tube and centrifuged at 373 g for 5 minutes. The supernatant was carefully removed completely and the cell pellet resuspended and mixed gently with chilled neutral collagen. The mixture was placed on top of the acellular layer of collagen at 50 µL/well. Where PTEC were cultured along with $CD4^+$ T cells, 200 µL of PTEC was mixed with 200 µL of T cells and centrifuged at 373 g for 5 minutes. The mixtures were plated at 50 µL/well in 96 well plates and allowed to polymerize for approximately 1 hr at 37 ˚C in the incubator. After the gels have formed 200 µL CM was added to each well and proliferation assay was performed as described in section 3.11.

3.4. Digestion of gels

PTEC and $CD4^+$ T cells were harvested from the collagen matrix by digesting enzymatically with 1 mg/ml collagenase P (Roche, Mannheim, Germany) in the presence of 20 µg/mL DNase I (Roche) for 15-20 mins at 37 ˚C. Cells were washed once with PBS and resuspended in medium for further study. This digestion protocol was also utilised for GelMA gels. The dissolution of alginate-based gels was carried out by addition of 500 µL of EDTA to the gels. The gels were incubated for 10-15 min to obtain cells. The cells were washed once in PBS at 373 g for 5 min before resuspending in CM for further study.

3.5. Flow cytometry

3.5.1. Cell surface staining

For surface staining of stimulated lymphocytes or PTEC, cells were washed once in FACS Buffer and subsequently incubated at 4 °C for 20 min with 30 µl of FACS Buffer containing appropriate dilutions of fluorochrome-conjugated antibodies or matched isotype controls optimised in our laboratory and previously published [3]. Briefly, recovered cells were resuspended in 30 µL FACS buffer (PBS + 0.5% bovine serum albumin (BSA) + 0.02% Sodium Azide) supplemented with 1 µL of each antibody and incubated at 4°C in the dark for 30 min. T cells were analysed by staining with fluorescein isothiocyanate (FITC), phycoerythrin (PE), and allophycocyanin (APC) conjugated monoclonal antibodies against CD4, CD69 and CD25 respectively. Conjugated mouse IgG1 and IgG2a served as isotype controls. For PTEC, cells were stained with APC and PE-Cy7 conjugated with monoclonal antibodies against HLA-DR and PD-L1 respectively. The isotype controls were conjugated mouse IgG1 and IgG2 antibodies. Following staining, the cells were washed in FACS Buffer and resuspended in 200 µl FACS Buffer for analysis within 2 h or 1 % paraformaldehyde (PFA; Sigma) supplemented PBS for delayed analysis. For viability staining, cells were labelled with the dead cell stain Near-IR (Life-technologies) according to the manufacturer's instructions and then acquired by flow cytometry. Viable cells stained negative for Near-IR.

3.5.2. Flow Data acquisition and analysis

Cell acquisition was carried out using BD Canto II flow cytometer (BD Biosciences) and analysis of flow data performed using FlowJo 10.1 (TreeStar).

Expression of an antigen was measured as the 'fold mean fluorescence intensity (MFI)', which is the change in MFI between a test antibody-stained sample and an isotype control-stained sample.

3.6. Expression of PD-L1 and MHC II PTEC cultured within 3D collagen gels

The effects of the cytokines IFN-γ and TNF-α and both together on the expression of PD-L1 and MHC Class II on primary human PTEC were studied.

Primary human PTEC ($4x10^4$ cells/well) were cultured within 3D collagen gels (for gel making refer section 3.3.3) for 36 hours following exposure to the cytokines. Duplicate cultures were established in a 96 well flat-bottom plate. No cytokine was added to the first two wells and acted as the control. PTEC in the next duplicate wells were exposed to IFN- γ (100 ng/mL). In two other wells PTEC were exposed to TNF-α (20 ng/mL). The final duplicate wells were exposed to IFN-γ (100 ng/mL) and TNF-α (20 ng/mL) together. A 2D culture with a similar set up was established at the same time. DM was used for PTEC culture.

After 36 hours, 2D cells were gently detached with TrypLE™ Express (1x) neutralized with trypsin inhibitor while 3D gels were digested (refer section 3.4) to harvest the cells. Cells were washed once in DM and re-suspended in FACS buffer for cell staining (refer 3.5.1) and acquired with flow cytometry. Data was analysed using FlowJo software.

3.7. CFSE labelling of $CD4^+$ T cells

To enable live cell imaging and to monitor cell division, freshly isolated $CD4^+$ T cells (refer 3.2.12) were labelled with carboxyfluorescein diacetate succinimidyl ester (CFSE). Briefly, 1 µM CFSE was prepared in PBS and an equal volume of cell suspension diluted to 2 x 10^6 cells/ml in PBS was added to it. The mixture was vortexed and incubated at room temperature for 5-10 mins with occasional shaking. After incubation, an equal volume of FCS was added to the mixture and centrifuged at 1400 rpm for 5 mins. Cells were then washed twice with RPMI-10 % FCS, counted in a haemocytometer (refer 3.2.13) and encapsulated in GelMA (refer 3.3.2) or collagen (refer 3.3.3) for live imaging.

3.8. Time-lapse video microscopy

Time lapse movements of PTEC and CFSE labelled $CD4^+$ T cells embedded in different types of gel constructs were recorded over a period of 20 hours or more using the Cell Voyager CV1000 Confocal Scanner Box (Yokogawa Electric Corporation). Live images of the cells were captured every 10 minutes using both brightfield and fluorescence channels. Z-stack (~ 7 μm z-steps) images were obtained.

Cells were tracked using the manual tracking option of Image J software (NIH, USA). The displacement of a cell was calculated by subtracting the positions between two time points.

3.9. Cell Viability in different gel models

To evaluate cell viability, PTEC and T cells encapsulated in gels were stained with fluorescein diacetate (FDA) for live cells and propidium iodide (PI) (both Invitrogen) for dead cells. Hydrogel constructs were transferred into a new 48 well plate and washed in PBS for 5 min at 37 °C. The gels were then incubated in PBS containing 10 μg/mL FDA and 5 μg/mL PI for up to 45 min at 37 °C and washed again with PBS for 5 min. Images were taken with either a confocal (Leica Microsystems, Wetzlar, Germany) or an Olympus microscope.

3.10. PTEC and $CD4^+$ T cells staining on GelMA

PTEC seeded on GelMA gels were grown for 28 days. At day 28, the gels were removed from the media, cut in half and transferred into 48 well plates. After fixation with 500 μL 4% paraformaldehyde (PFA) for 20 mins at room temperature the gels were washed twice with PBS for 5 mins and the cells within the gels were stained for different markers as follows:

3.10.1. Staining with vimentin antibody, DAPI (4′, 6-diamidino-2-phenylindole dihydrochloride) and PNA (lectin- peanut agglutinin)

As we would expect cells to undergo epithelial to mesenchymal transition (EMT) in long term cultures, PTEC cultured for 4 weeks on gelMA were tested for EMT by staining with vimentin.

For intracellular staining of vimentin, cells within gels were permeabilized by incubating with PBS containing 0.1 % Triton-X100 for 20 mins. Next, gels were washed for 5 min with PBS and 250 µL of primary antibody solution was applied. The primary antibody solution constituted of mouse anti-human vimentin antibody (IgG1κ) final concentration 4.9 µg/mL in 3 % (v/v) donkey serum/PBS. After an hour of incubation at RT, samples were washed twice with 500 µL of PBS for 5 mins on a shaker. Secondary antibody solution comprising of DAPI (final concentration 5 µg/mL), Alexa Fluor® 488 –labelled donkey anti-mouse antibody (final concentration 4.7 µg/mL) and PNA (final concentration of 20 µg/mL) in 3 % donkey serum/PBS was added to gels for 1 hour in the dark. At the end of incubation time, gels were washed twice in ice-cold PBS for 5mins on a shaker and images taken on a confocal microscope (SP5 Leica).

3.10.2. Staining with rhodamine phalloidin, DAPI and PNA

Following fixation, gels were incubated with 250 µL antibody solution comprising of DAPI (final concentration 5 µg/mL) rhodamine phalloidin (0.8 U/mL) and Alexa fluor ® 647 labelled lectin PNA (20 µg/mL) in PBS. After an hour of incubation at room temperature (RT), samples were washed twice with 500 µL of PBS for 5 mins on a shaker and images taken on a confocal microscope (SP5 Leica).

3.10.3. Staining with collagen IV antibody, E-cadherin antibody and DAPI

After the gels were fixed and washed in PBS, a solution of primary antibodies against E-cadherin (1 in 200 dilution) and collagen IV (3.5 µg/mL) in PBS containing 3% donkey serum was added to the gels and incubated at RT for 1 hour. Next, samples were washed twice with PBS for 5 mins on a shaker before a

secondary antibody mix of DAPI (final concentration 5 µg/mL), Alexa Fluor ® 594 – labelled donkey anti–rabbit secondary antibody and Alexa Fluor ® 488 – labelled donkey anti-mouse antibody (both at final concentration 4.7 µg/mL) was applied to the gels. Gels were incubated 1 hr in dark at RT and washed twice with ice cold PBS. Images were taken on a confocal microscope (SP5 Leica).

3.11. Proliferation assays

2D cultures were established in flat-bottom 96-well plates with $CD4^+$ T cells at 2×10^5/ well with or without IFN-γ-activated (100 ng/mL), irradiated (30 Gy) PTEC, at a concentration of 1.5×10^5/mL.

For 3D cultures, an acellular layer of collagen type I was laid to the bottom of wells of a 96 flat-bottom plate. The same number of $CD4^+$ T cells and PTEC were mixed with 50 µL of collagen solution and added to the appropriate wells (refer section 3.3.3). CM was added to all wells. Cultures were established in triplicate with the following stimulator concentrations: phytohaemagglutinin (PHA) 20 µg/mL, mouse anti-human CD3 clone CLB-T3/4.E (αCD3) 0.5 µg/mL and mouse anti-human CD28 clone CLB-CD28/1 (αCD28) 0.1 µg/mL. Cultures containing PHA and αCD3/28 were incubated for 3 days at 37 °C in 5 % CO_2. Proliferation was assessed by the addition of 1 µCi 3H-thymidine/ well for the last 8 h of cultures. 3D gels were dissolved (refer section 3.4) and cells were harvested using a Skatron Cell Harvester. Results are expressed as a stimulation indices (SI), obtained by dividing means of triplicate test wells by means of relevant triplicate no stimulation control wells.

3.12. PTEC-T cell blocking studies

In order to identify the mechanism behind the immuno regulatory role of autologous PTEC, surface molecules such as PD-L1 and intracellular IDO were neutralised within the PTEC-T cell co-cultures. In 2D cultures and 3D cultures, PD-L1 was blocked by addition of 10 µg/mL of anti-human PD-L1 (Bio legend, San Diego) blocking antibody to the surface of PTEC and incubated for 2 h at 37ºC. Following incubation, the PTEC wells were washed to remove excess antibody and

the co-cultures were established as described in section 3.11. To neutralise IDO, 1500 µM/mL IDO inhibitor 1-MT was added into the PTEC or control wells following the set-up of co-cultures.

3.13. Chemokine Analysis

Chemokines CXCL8/IL-8, CCL5/RANTES, CXCL9/MIG (Monokine induced by gamma interferon), CCL2/MCP-1 and CXCL10/IP-10 (Interferon gamma-induced protein 10) were analysed from PTEC culture supernatants using Cytometric Bead Array Human chemokine kit (BD Biosciences) according to manufacturer's instructions. Briefly, standard chemokine dilutions were performed as per instructions in the manual. 50 µL of standard solutions and samples were added to different wells of a 96 well U-bottom plate. To these wells 50 µL of mixed capture beads were added. This was followed by addition of 50 µL of Human Chemokine PE Detection Reagent to the wells. The plate was incubated for 3 hours at RT, protected from light. Each well was topped-up with 150 µL of wash buffer and centrifuged at 200 x *g* for 5 min. The supernatant was discarded and pellet was resuspended in 100 µL of wash buffer. Samples and standards were acquired using FACS array (BD Biosciences). Data analysis was done on FCAP array software (BD Biosciences).

3.14. Cytokine Analysis

3.14.1. Human Inflammatory Cytokines

Human inflammatory cytokines IL-8, interleukin-1-β (IL-1β), interleukin-6 (IL-6), interleukin-10 (IL-10), tumor necrosis factor (TNF) and interleukin-12p70 (IL-12p70) within supernatants from 2D and 3D cultures were measured using Cytometric Bead Array Human Inflammatory cytokines kit (BD Biosciences) according to manufacturer's instructions (section 3.13).

3.14.2. Human Th1/Th2 Cytokine Kit II

Human Th1/Th2 cytokines interleukin-2 (IL-2), interleukin-4 (IL-4), IL-6, IL-10, TNF and IL-12p70 within supernatants from 2D and 3D cultures were measured

using Cytometric Bead Array Human Th1/Th cytokine kit (BD Biosciences) according to manufacturer's instructions (section 3.13).

3.15. Collaborations

A/Prof. Travis Klein and Dr. Karsten Schrobback from IHBI at QUT have collaborations with Dr. Ray Wilkinson from the Conjoint Renal Research Lab at QIMR Berghofer to work on this project together using facilities available at both IHBI and QIMR Berghofer. Dr. Helen Healy (Head of Renal Research Lab) and Dr. Ray Wilkinson from the Conjoint Renal Research Laboratory, Queensland Health have approval to obtain kidney tissue and blood from patients undergoing nephrectomies at the Royal Brisbane and Women's Hospital, Wesley Hospital.

3.16. Statistical Analysis

Comparisons between groups were performed using two-tailed *t*-test. Statistical tests were performed using GraphPad Prism 6.0 analysis software (GraphPad, San Diego, CA). P-values ≤ 0.05 were considered statistically significant.

3.17. Ethics and Limitations

This project had ethics approval from The Queensland Institute of Medical Research - Human Research Ethics Committee (QIMR-HREC Ref. No. P293), The Royal Brisbane and Women's Hospital -Human Research Ethics Committee (RBWH-HREC Ref. No. 2002/011), Queensland Health-Pathology (Ref. No. P293RB) and the Wesley Research Hospital Tissue Bank.

Chapter 4: Results

4.1. Defining a 3D matrix suitable for PTEC and T cell co-culture.

4.1.1. Gel mixtures as a matrix to co-culture PTEC and CD4$^+$ T cells.

Various hydrogels and hydrogel combinations were examined to define a suitable matrix for 3D culture of PTEC and CD4$^+$ T cells. To increase matrix stiffness and improve handling, alginate was added to either collagen or Matrigel. These mixtures of gels were then used to encapsulate CD4$^+$ T cells and viability of cells was checked at different time points.

Live-dead staining of CD4$^+$ T cells at 24 hours into culture indicated that the alginate only gels had lower viability compared to the alginate-collagen and alginate-matrigel gels (**Figure 4.1**).

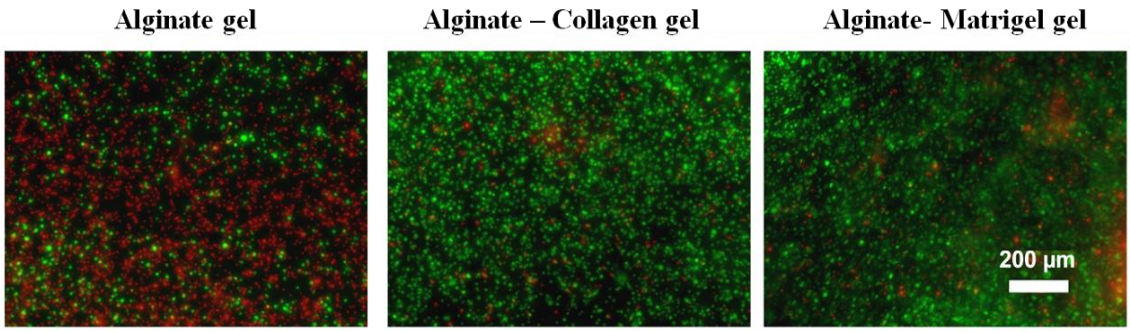

Figure 4.1 Live and dead staining of encapsulated CD4$^+$ T cells in different combinations of gels.

At 24 hrs into culture, CD4$^+$ T cells within the different gel types were stained with fluorescein diacetate (FDA) and propidium iodide (PI) to detect live (green) and dead (red) cells. Cells encapsulated within alginate only gel had lower viability compared to the alginate-collagen and alginate-matrigel gels.

The alginate-collagen and alginate–matrigel gels were cultured for a week and stained for live and dead cells. Images taken at day 7 after staining demonstrated a major decrease in viability in both alginate-collagen gel and alginate-matrigel gel compared to day 1 (**Figure 4.2**).

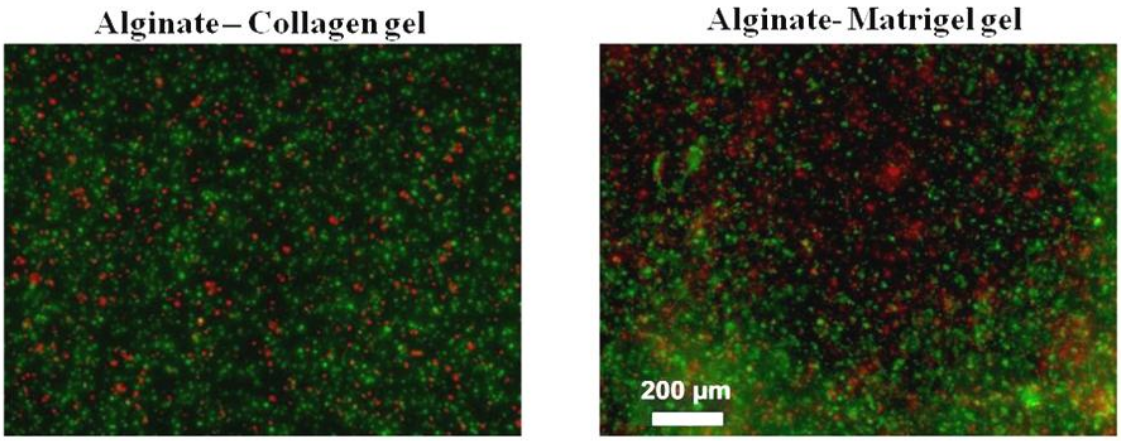

Figure 4.2 **Live and dead staining of encapsulated purified CD4$^+$ T cells in different gels after 7 days in culture.**

The cells were stained with fluorescein diacetate (FDA) and propidium iodide (PI) to detect live (green) and dead (red) cells.

4.1.2. Gelatin methacrylamide (GelMA) as a 3D matrix to co-culture PTEC and CD4$^+$ T cells.

4.1.2.1.PTEC attachment and viability on GelMA hydrogel

GelMA hydrogel has been shown to be able to sustain long term viability of different cell types [110, 115].

To demonstrate whether GelMA is a suitable hydrogel to sustain PTEC, these cells were seeded on 5% GelMA and cultured for 8 days. Images were taken at day 8 with a brightfield microscope. In 3D culture formation of network and tubule-like structures were seen whereas in 2D cultures the cells formed a confluent monolayer of cells **Figure 4.3.**

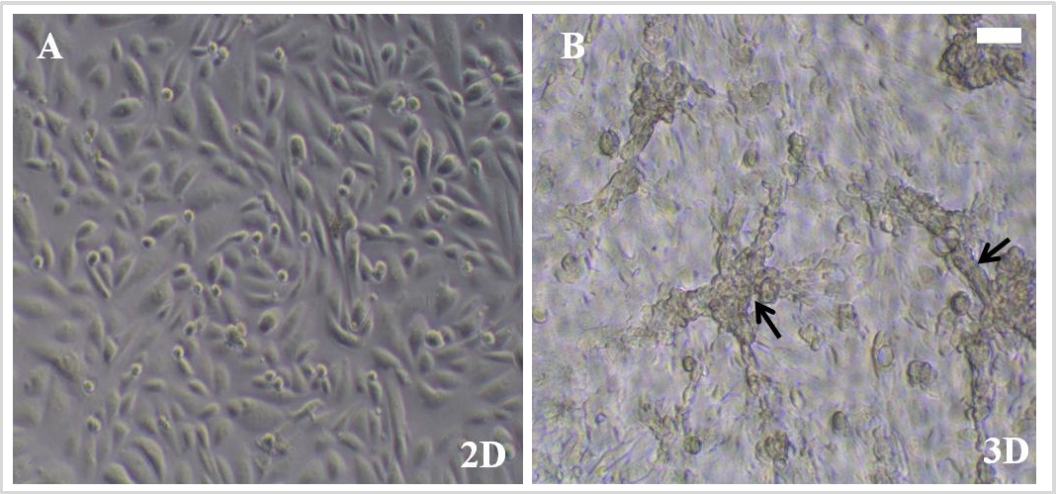

Figure 4.3 (A) PTEC at day 8 in 2D culture (B) PTEC in 3D culture (seeded on 5 % GelMA) at day 8.

Formation of networks and multicellular structures (black arrows) were seen in 3D culture. Images were taken with Olympus CK40 (Scale bar = 100µm).

Purified $CD4^+$ T cells were encapsulated in 5% GelMA and PTEC were seeded on the GelMA hydrogel. Following 4 weeks in culture, the cells were stained for actin filaments (phalloidin-green), glycosylated proteins (peanut agglutinin-red) and nuclei (DAPI-blue). Confocal images were taken at day 28. Figure 4.4**Error! eference source not found.** shows network formation by PTEC on GelMA. However, no T cells were detected within the GelMA at day 28.

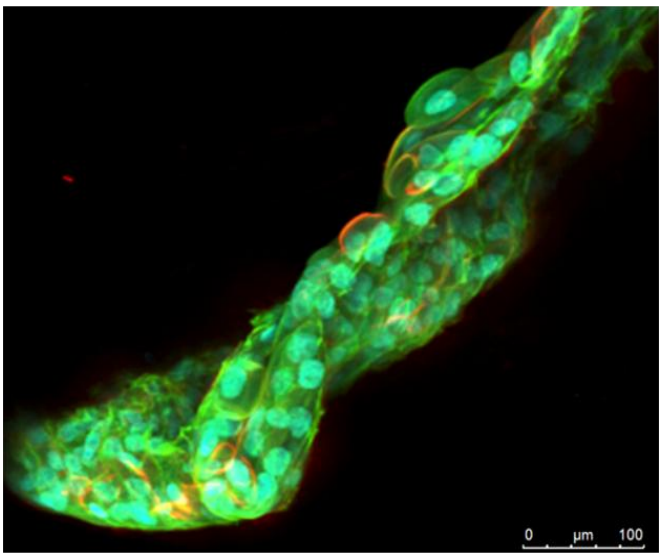

Figure 4.4 Confocal image of purified CD4+ T cells and PTEC on GelMA 3D at day 28.

Cells are stained for actin filaments (phalloidin-green), glycosylated proteins (Peanut agglutinin-red) and nuclei (DAPI-blue). No Live T cells were detected.

PTEC on GelMA 3D hydrogel cultures stained positive for epithelial cell marker E-cadherin, which were visualised with confocal immunoflourescence, with nuclei stained with 4', 6-diamidino-2-phenylindole (DAPI) **Figure 4.5.**

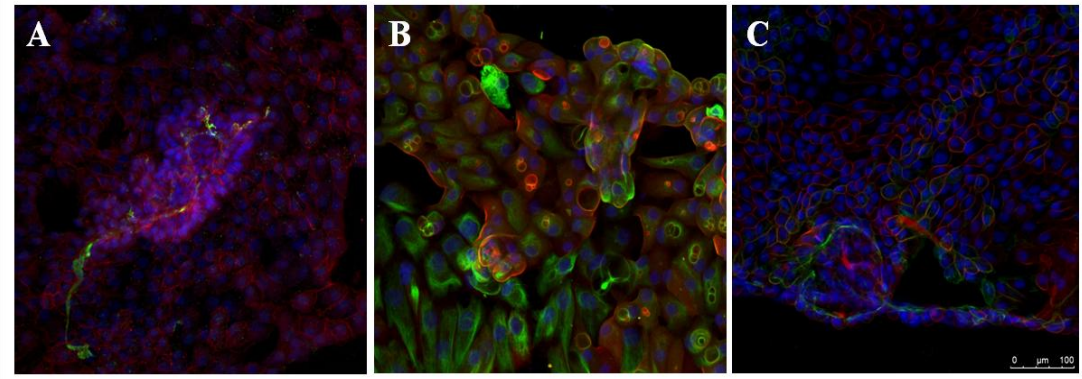

Figure 4.5 PTEC expressed typical epithelial cell markers on GelMA 3D hydrogel cultures which was visualised with confocal immunofluorescence.

(A) PTEC stained positive for E-cadherin (red) and nuclei (DAPI-blue) , collagen IV (green), (B) PTEC stained positive for vimentin (green), PNA (red) and nuclei (DAPI-blue), (C) Phalloidin (green), PNA (red) and DAPI (blue).

PTEC grown on the GelMA surface remained viable for at least 4 weeks in culture forming networks and spreading to cover the hydrogel surface.

4.1.2.2. Effect of brief UV exposure on $CD4^+$ T cells.

The ability of $CD4^+$ T cells to migrate and remain viable within GelMA hydrogels was examined. GelMA requires approximately 5 minutes of ultraviolet (UV) radiation to form a gel. To test the effect of UV exposure on $CD4^+$ T cell viability, purified $CD4^+$ T cells were added to a glass slide chamber and exposed to UV for 5 mins. A control was set up by adding an equal number of purified $CD4^+$ T cells into another glass slide chamber. Viability of the cells at different time points was tested by staining the cells with a Near Infrared (IR) dye and analysing using flow cytometry. As shown in **Figure 4.6**, the flow cytometry profile (**A & B**) of the T

cells at day 3 suggested that 5 min UV exposure does not affect viability of $CD4^+$ T cells. The percentage viability of both the control and UV-exposed T cells (**Figure 4.6 C**) was similar over 6 days.

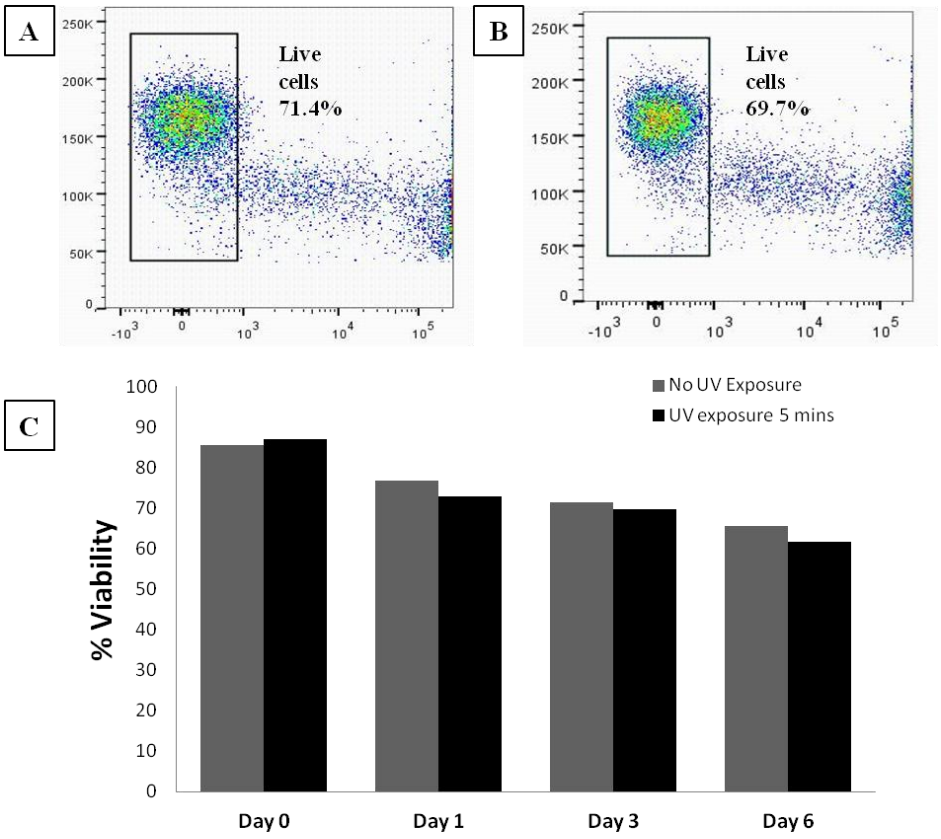

Figure 4.6 Effect of brief UV exposure on $CD4^+$ T cell viability

A) Typical flow cytometry profile from control and (B) UV-exposed $CD4^+$ T cells at day 3. (C) Control $CD4^+$ T cells (grey bars) and cells exposed to UV for 5 min (black bars) were cultured in complete media for 6 days and their viability monitored at days 1, 3 and 6 by staining with the viability dye Near IR (stains dead cells) and analysing using flow cytometry. Data shows results of n=1.

4.1.2.3. Ability of encapsulated $CD4^+$ T cells to remain viable and migrate within GelMA.

The ability of encapsulated T cells to successfully migrate within GelMA gel was studied. T cells are highly motile cells that constantly circulate in the blood. These cells migrate into different organs in response to injurious stimuli to mediate immune responses.

Time lapse photography of $CD4^+$ T cells (labelled with CFSE) within GelMA gel over a period of 20 hours demonstrated no movement of T cells through the gel (**Figure 4.7)**.

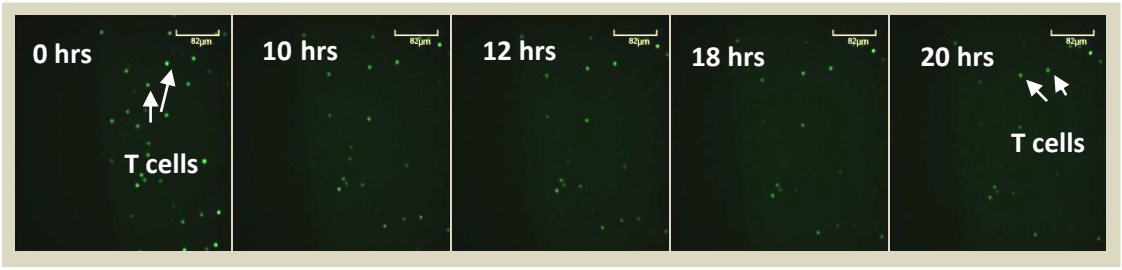

Figure 4.7 Live cell images of CD4+ T cells in GelMA gel.

Freshly isolated CD4+ T cells were pre-labelled with CFSE and encapsulated in GelMA. Time lapse photography of CD4+ T cells (green) in GelMA gel over a period of 20 hours shows no T cell movement through the gel.

The number of viable $CD4^+$ T cells over time in GelMA was estimated based on CFSE staining. CFSE positive cells were counted in one field of the images. Images were taken every 10 mins and 28 live T cells were present in the field at start. **Figure 4.8** suggests that the number of live $CD4^+$ T cells in GelMA declined over time.

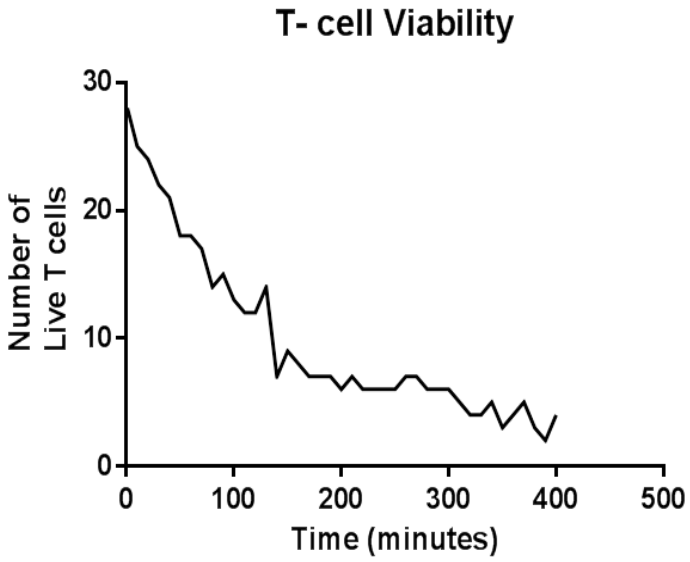

Figure 4.8 Viability of $CD4^+$ T cells in GelMA gel.

Viability of encapsulated T cells was determined from the live images captured using a confocal microscope (Cell Voyager CV-1000). Purified CD4+ T cells were CFSE labelled before encapsulating within GelMA. Images were taken every 10 mins using the fluorescence channel. Based on CFSE staining, cells were counted from one field of image. Number of live T cells in the field was 28 at start but this decreased over time.

To further confirm the findings, PTEC and T cells were encapsulated within 5 % GelMA gel and their viability examined at day 5. **Figure 4.9** shows that PTEC remained viable when encapsulated within GelMA but all $CD4^+$ T cells were dead after 5 days in culture within the GelMA culture model.

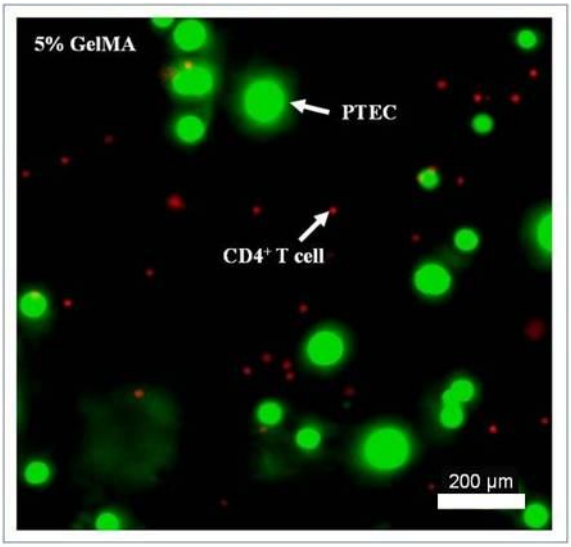

Figure 4.9 PTEC and CD4+ T cells encapsulated in GelMA.

The cells differentiated by size were stained with fluorescein diacetate (FDA) and propidium iodide (PI) to detect live (green) and dead (red) cells. Images were taken at day 5 using Olympus IX81.

4.1.3. Collagen type I as a matrix for co-culture of PTEC and $CD4^+$ T cells.

Collagen is one of the vital components of the ECM in natural tissue. To successfully use collagen as a matrix for co-culturing of autologous primary human PTEC and immune cells, the ability of T cells to migrate and interact with PTEC within collagen was examined.

T cell migration within collagen gel was assessed by performing live–cell imaging. Time lapse video-microscopy of encapsulated T cells showed that T cells were capable of effectively migrating through the gel (refer video 1). **Figure 4.10** shows T cell movement through collagen using manual tracking (Image J software) over a period of 20 hours.

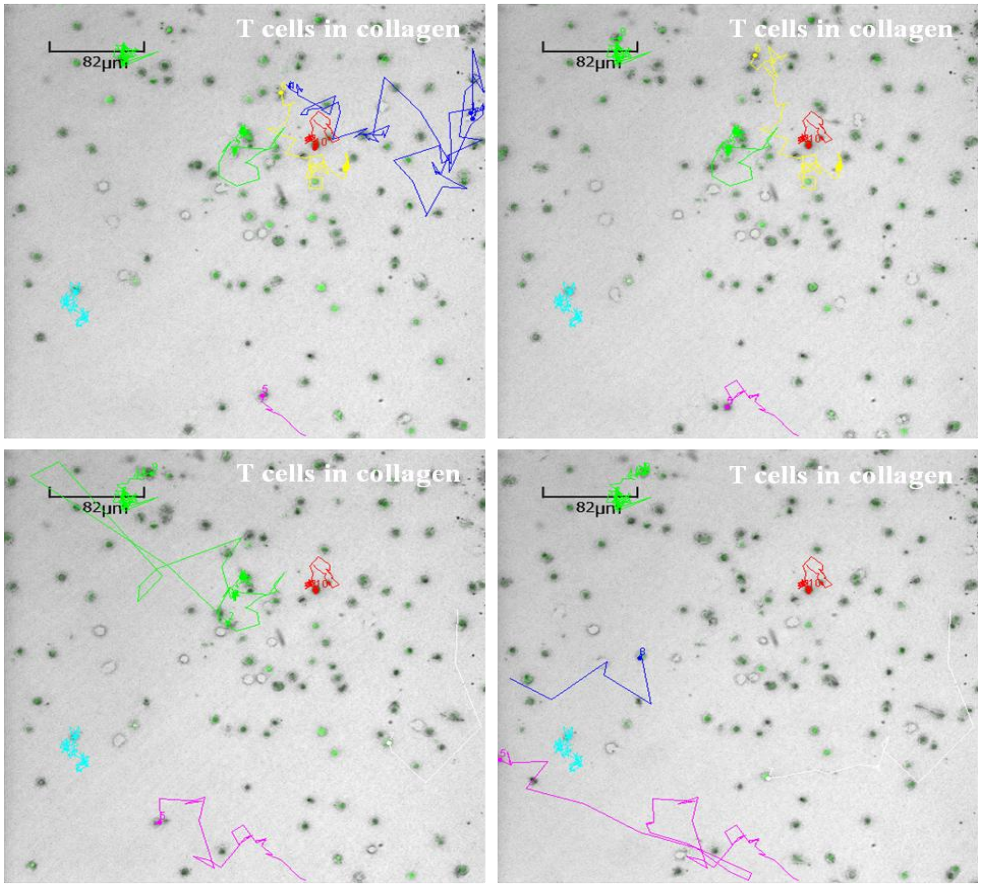

Figure 4.10 Encapsulated T cell movement through collagen gel.

T cells were pre-labelled with CFSE and encapsulated within collagen gels and imaged live over 24 h using the CV1000 Confocal Scanner Box (Yokogawa Electric Corporation). Cells were tracked using Image J software. The paths followed by individual T cells are plotted as colored lines. The different images show different T cells tracked within the same gel. When a particular T cell disappeared from the field its path was omitted in the succeeding images.

To evaluate the capability of PTEC to move through the collagen gel, PTEC were encapsulated within collagen and imaged live (with CV 1000 Confocal Scanner Box, Yokogawa Electric Corporation) over 24 hours. PTEC tracking within collagen gel using Image J software (**Figure 4.11**) revealed that these cells were capable of spreading and multiplying (seen in videos taken beyond 24 h, data not shown here) within collagen.

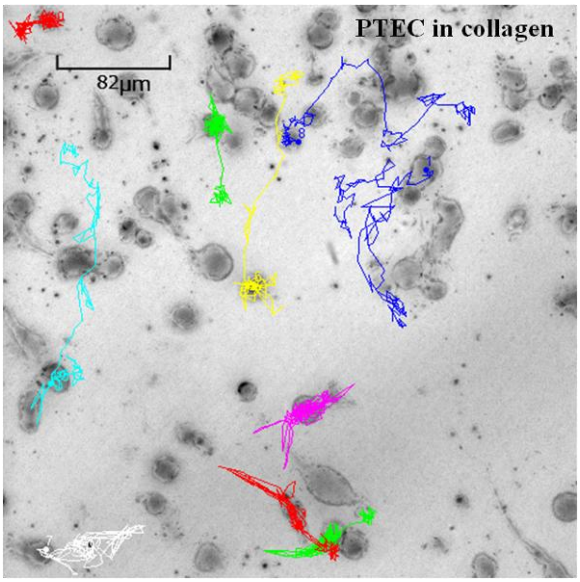

Figure 4.11 PTEC movement through collagen.

PTEC were encapsulated within collagen gels and imaged live over 24 h using the CV1000 Confocal Scanner Box. Cells were tracked using Image J software. Ten individual PTEC were tracked within the collagen gel and colored lines indicate paths followed by PTEC over 24 h.

The next objectives were to record movements of T cells in presence of PTEC and visualize their interactions within collagen gels. To accomplish this, PTEC and T cell were encapsulated within collagen gels together and their time lapse movement recorded over 24 hours. Images showed that both cell types were capable of moving through the gel and interacting with each other. When T cells were tracked in presence of PTEC within collagen gels (**Figure 4.12**) their movement within the gel appeared to some extent restricted when compared to movement of T cells alone within collagen. In order to investigate this further, two separate analyses were undertaken.

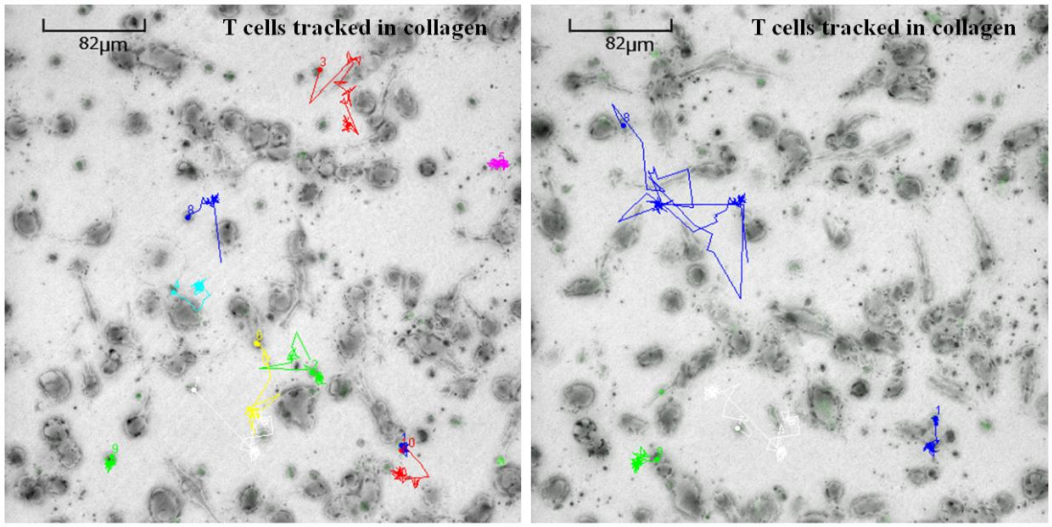

Figure 4.12 T cell tracking within collagen gels in presence of PTEC.

PTEC and CD4+ T cells were encapsulated within collagen gels and imaged live using CV 1000 Confocal Scanner Box. T cells were tracked using Image J software. The paths followed by individual T cells are plotted as colored lines. The two images show different T cells tracked within the same gel. When a particular T cell disappeared from the field its path was omitted in the succeeding images.

Mean T cell displacements in absence or presence of PTEC were plotted as a function of the square root of time. A plot of mean displacement of cells against the square root of time provides some information about the type of migration that is involved. Results from this methodology are presented in **Figure 4.13**. However, from these results it is difficult to interpret whether the migration represents a "random walk" or a directional movement. What can be inferred from the results presented in **Figure 4.13** is that in the presence of PTEC T cells displayed an obvious restricted mobility, suggesting cellular interaction [123].

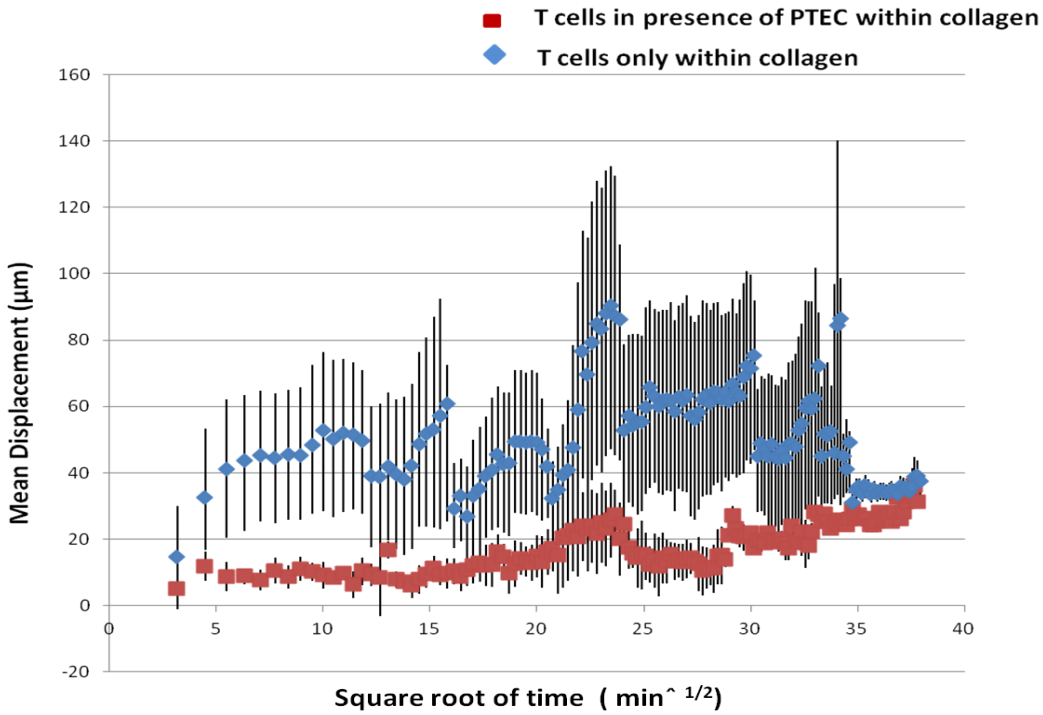

Figure 4.13 Mean displacement of T cells in absence and presence of PTEC within collagen gels.

The second methodology utilised a track plot of T cell movement to obtain a qualitative indication of cell movement and directionality. This track plot is plotted by shifting the origin of each individual cell to the same point in space without changing their orientation. The plot also helps to roughly determine whether cells are undergoing a directional movement or a "random walk". A plot in which all possible directions of migration are covered is indicative of random movement [123]**. Figure 4.14** shows the track plots for T cells encapsulated within collagen in absence and presence of PTEC. The graphs are indicative of a random movement within the gel in absence of PTEC. However, in presence of PTEC, the plot suggests a preferred directional migration.

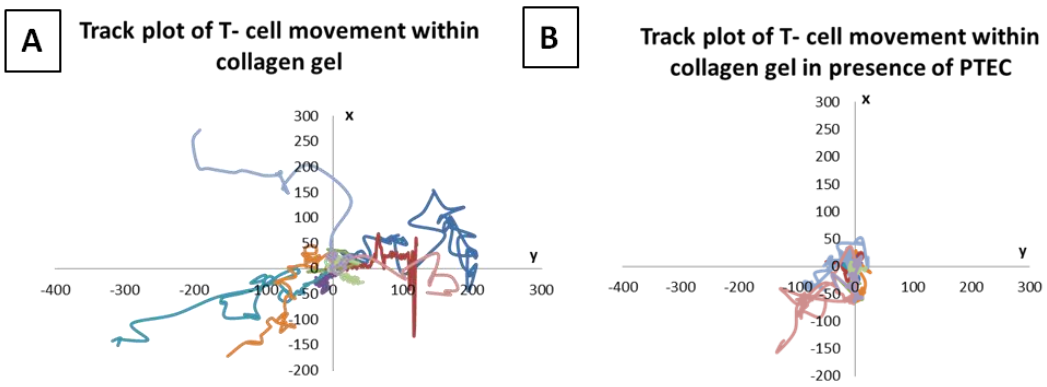

Figure 4.14 A track plot with tracks being shifted to start at the origin of x and y axes (A) shows the tracks followed by T cells within the collagen gel in absence of PTEC (B) shows track plots of T cells in presence of PTEC when both cells were encapsulated within the collagen gel.

The time lapse images from the videos (refer video 2) illustrated that T cells and PTEC within the collagen gel culture model were capable of moving through the gel. T cells moved rapidly through the gel and interacted with PTEC. The interactions arrested the movement of the T cells for a time span ranging from 2-4 hrs approximately. T cells migrated away from the PTEC after the interaction. **Figure 4.15** shows snapshots from a time lapse video illustrating movement and interactions of T cells and PTEC within the collagen culture model.

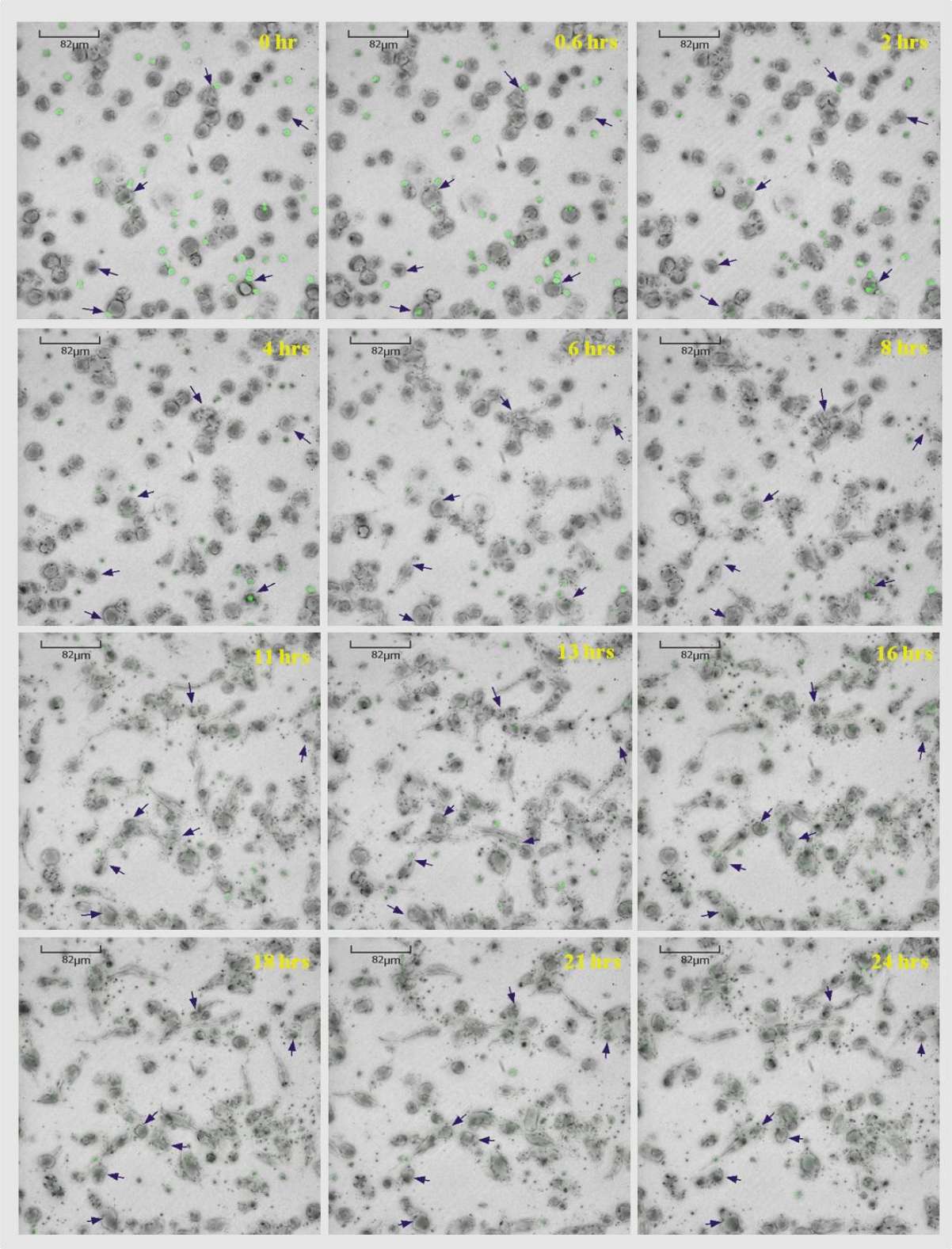

Figure 4.15 Snapshots from time lapse videos showing interactions and movement of T cells and PTEC within collagen gels.

PTEC and T cells (pre-labelled with CFSE) were encapsulated within collagen gels and live-cell imaging was performed for 24 h using CV1000 confocal scanner box. Black arrows indicate PTEC and T cells that had interactions.

4.1.4. Summary

Previously the interactions between autologous PTEC and T cells were studied using 2D static *in vitro* cultures. In an attempt to design a 3D *in vitro* model to investigate the interactions of these two types of cells under a more physiologically relevant condition, various types of 3D cell culture models were investigated.

In the first instance, alginate and $CD4^+$ T cell interactions were monitored. Alginate gels are to some extent similar to ECM in tissues but lack cell adhesion sites and allow no interaction between the gel and the cells [92]. I found that a significant number of encapsulated T cells died within the first 24h. To add adhesion sites for the cells within alginate gel, it was either mixed with collagen or Matrigel. T cells were then encapsulated into mixtures of alginate-collagen and alginate–matrigel and cultured for a week. Live/Dead staining of cells in these gels at day 7 indicated that there were again numerous dead cells. All the results suggested that alginate gel or mixtures of alginate gels with ECM-based materials were not suitable for the long-term maintenance of human T cells.

Next GelMA hydrogel was examined as a possible ECM for co-culturing PTEC and T cells. PTEC showed promising results when cultured on GelMA hydrogel. Following a week of PTEC culture on GelMA the cells formed networks and multi-cellular structures in the 3D model. PTEC also expressed epithelial cell marker when cultured for 4 weeks on GelMA. As GelMA is a photo-cross linkable gel the effect of brief UV exposure on the T cell viability within GelMA was examined. Results suggested that brief exposure of UV does not affect viability of T cells within GelMA. However, the ability of T cells to migrate within GelMA appeared restricted and T cells were incapable of migrating through the 3D GelMA culture model.

Collagen is one of the vital components of the ECM. Research has shown that the pattern of migration of leukocytes in 3D collagen closely resembles the *in vivo* leukocyte migration in peripheral tissues. [124]. In this thesis collagen was next tested as a potential 3D matrix for the co-culture of cells. Within this collagen model, T cells were capable of migrating through the gel. PTEC were able to migrate and spread within the collagen gel. The collagen gel model was

able to sustain both the PTEC and T cells and there were interactions between T cells and PTEC.

4.2. Activated PTEC modulate CD4$^+$ T cell responses in a 3D *in vitro* model

4.2.1. Expression of activation markers on CD4$^+$ T cells in 3D collagen culture

The expression of activation antigens on CD4$^+$ T cells within collagen gels was monitored. CD4$^+$ T cells were stimulated with anti-CD3/28 in gels and after 3 days in culture, the gels were dissolved and recovered T cells stained for surface expression of CD69 and CD25 antigens. The cells were analysed using flow cytometry. CD4$^+$ T cells increased the expression of their activation markers within collagen gel following stimulation (**Figure 4.16**). Minimal to no expression of activation markers CD69 and CD25 were seen on unstimulated CD4+ T cells.

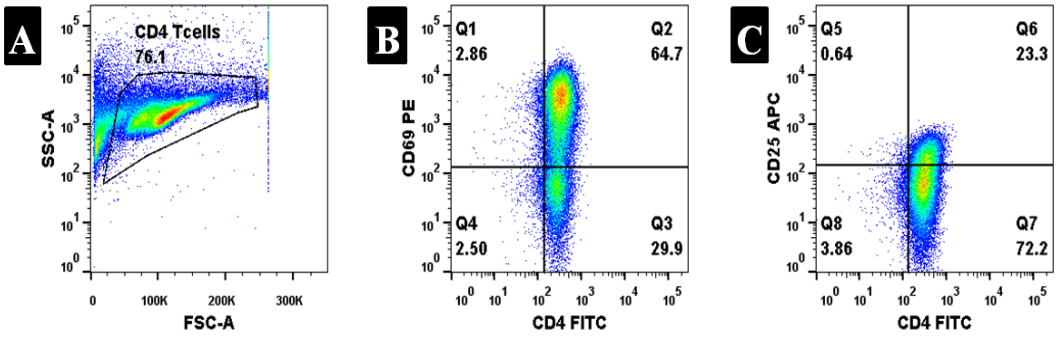

Figure 4.16 Expression of activation markers CD69 and CD25 on CD4 $^+$ T cells in 3D collagen gels after being stimulated with anti-CD3/28.

(A) Forward and side scatter profiles of CD4 $^+$ T cells extracted from 3D gels. (B) Expression of CD69 and (C) expression of CD25 on T cell surface extracted from 3 D gels.

4.2.2. Surface antigen expression of PTEC in the presence of inflammatory cytokines in 2D and 3D *in vitro* cultures.

Initially, PTEC from one donor were cultured for 36 h in a 3D collagen gel culture system in the presence of 100 ng/mL gamma-interferon (IFN-γ), 20 ng/mL of tumour necrosis factor (TNF-α) and a combination of 100 ng/mL IFN-γ and 20 ng/mL of TNF-α to determine whether these cells could up-regulate their surface expression of PD-L1 and MHC class II (HLA-DR). After 36 h, gels were digested and the recovered cells stained for these antigens. Results demonstrated that there was maximum up-regulation of these antigens in response to IFN-γ and TNF-α combined (**Figure 4.17**), confirming that PTEC within 3D collagen gels were capable of up-regulating their surface antigen expression.

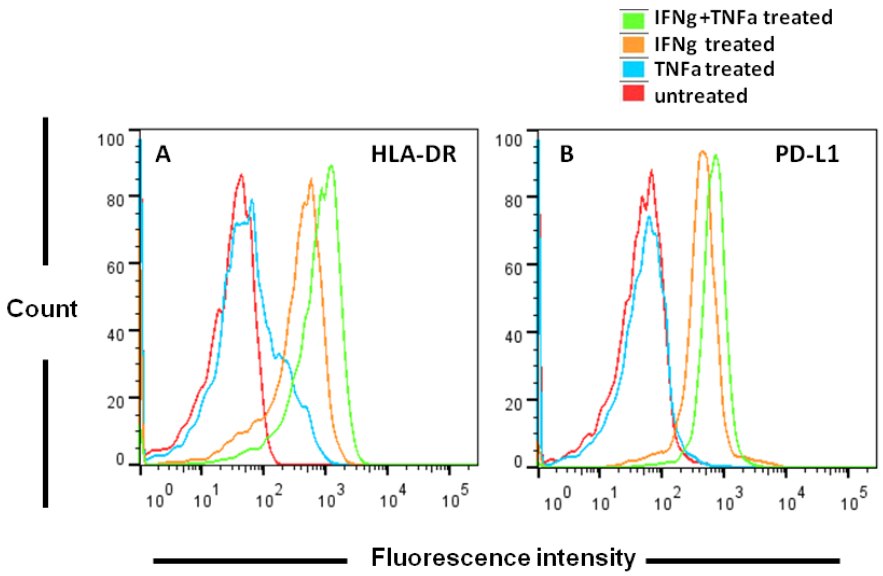

Figure 4.17 Inflammatory cytokine induced PD-L1 and HLA-DR expression on primary PTEC cultured using the 3D *in vitro* model.

A and B shows the expression of HLA-DR and PD-L1, respectively, in a representative donor. PTEC were encapsulated within collagen gels and cultured for 36 h in presence of 100 ng/mL gamma-interferon (IFN-γ) , 20 ng/mL of tumour necrosis factor (TNF-α) and a combination of 100 ng/mL IFN-γ and 20 ng/mL of TNF-α in different wells. After 36 h the gels were digested to recover the cells. PTEC were next stained for PD-L1 and HLA-DR and surface expression checked by flow cytometry.

Our group has previously demonstrated, using 2D culture, that IFN-γ exerts a major up-regulation of PD-L1 and HLA-DR expression on primary human PTEC

[3]. Therefore, the differences of surface antigen expression of PTEC cultured in 2D and 3D systems were then compared. Primary human PTEC from two different donors were subjected to 36-h exposure to the inflammatory cytokines in 2D and 3D cultures. As seen in **Figure 4.18**, the delta mean fluorescence intensity (ΔMFI) for the expression of PD-L1 and HLA-DR suggested that in both the donors there were higher expressions of these molecules on activated PTEC in 3D as opposed to 2D cultures.

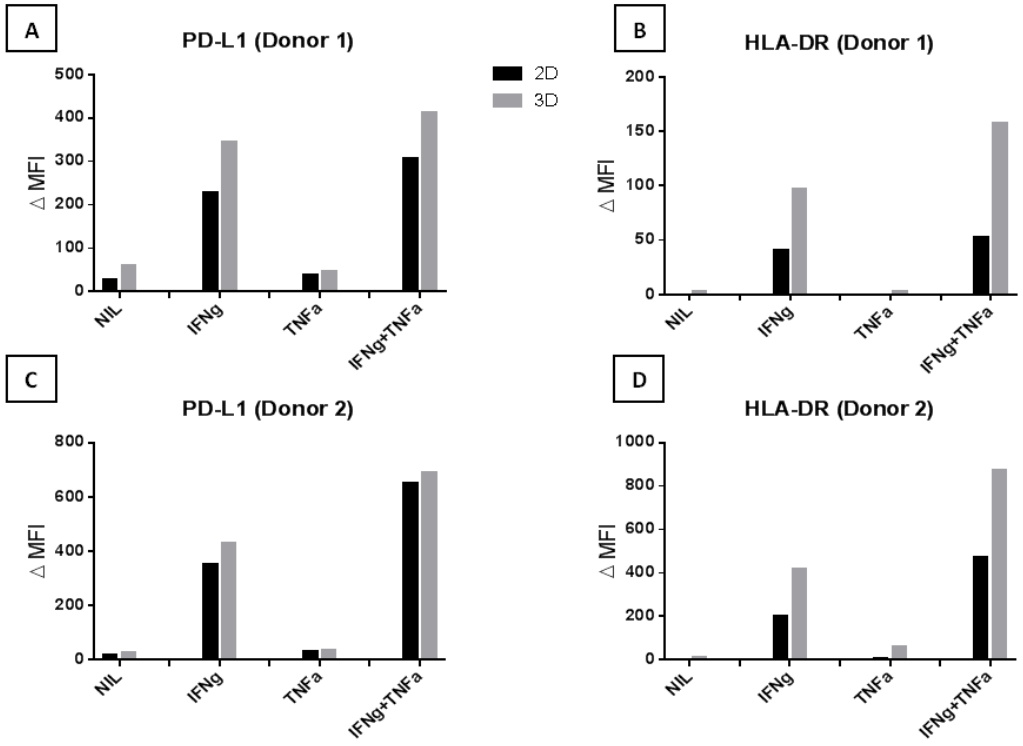

Figure 4.18 PTEC from two donors were stained for the expression of PD-L1 and Class II (HLA-DR) following 36 h exposure to 100 ng/mL gamma-interferon (IFN-γ), 20ng/mL of tumour necrosis factor (TNF-α) and combination of 100 ng/mL IFN-γ and 20 ng/mL of TNF-α.

Surface expression was measured by flow cytometry (gated on single, live cells) and expressed as the delta mean fluorescence intensity (ΔMFI) (MFI of test samples - MFI of isotype control). ΔMFI for the expression of PD-L1 and HLA-DR is shown for donor 1 in A and B respectively and for donor 2 in C and D respectively.

4.2.3. Modulation of proliferative responses by autologous PTEC in 2D and 3D.

Next, the ability of activated autologous PTEC to modulate the proliferation of purified $CD4^+$ T cells in response to PHA and anti-CD3/CD28 was compared using 2D and 3D *in vitro* cultures. The proliferation assay was repeated using 6-7 donors. **Figure 4.19** shows a greater down-modulation of $CD4^+$ T cell proliferation occurred within 3D cultures than those within 2D cultures. This result may provide support for the hypothesis that 3D culture models provide a more realistic *in vivo* environment than 2D cultures.

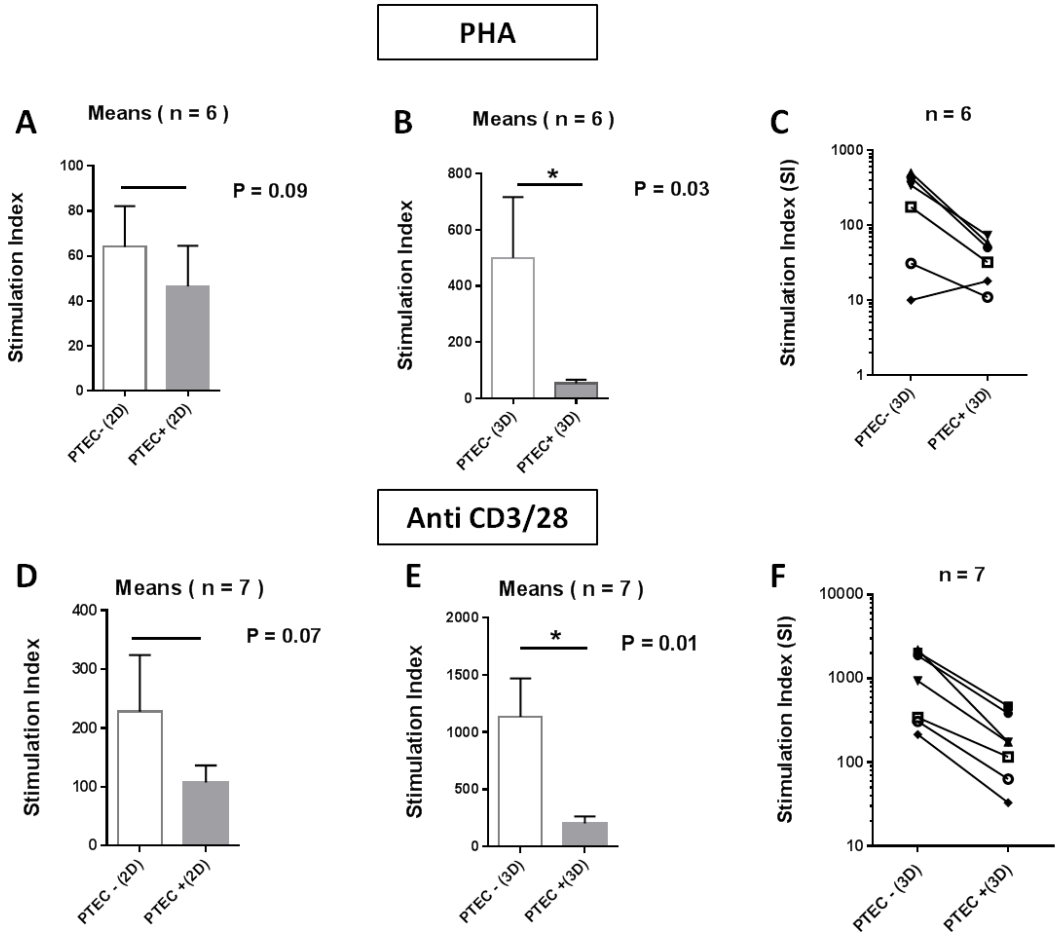

Figure 4.19 Activated PTEC suppressed proliferative responses of autologous T cell populations.

Activated PTEC suppress proliferative responses of autologous T cell populations. (A) and (B) show the means of 6 separate experiments ±1 SEM in 2D and 3D cultures respectively and (C) shows the results from all six donors in response to PHA in the 3D culture. (D) and (E) show the means of 7 experiments ±1 SEM in 2D and 3D cultures respectively and (F) shows the results of all seven donors in response to anti-CD3/CD28 in 3D culture. Results are expressed as Stimulation index (SI), obtained by dividing means of triplicate test wells by means of relevant triplicate no stimulation control wells. Statistical comparisons between two groups were performed using a two tailed *t* –test. * $P \leq 0.05$ when compared with no added PTEC.

4.2.4. Down-modulation of immune cell responses by activated autologous PTEC is partially mediated by PD-L1 in 3D cultures.

A previous paper published by our laboratory has demonstrated that in 2D cultures, down-modulation of immune cell responses by autologous activated PTEC is partially mediated by PD-L1 [3].

To examine the role of this molecule in immune-regulation within our 3D cultures, blocking studies were performed by addition of anti-PD-L1 (clone 29E.2A3) antibody (Ab) to PTEC encapsulating in the gels. The addition of anti-PD-L1 Ab showed partial recovery of proliferation in 3D co-culture experiments compared to the inhibition seen in the presence of PTEC without the blocking antibody (**Figure 4.20**).

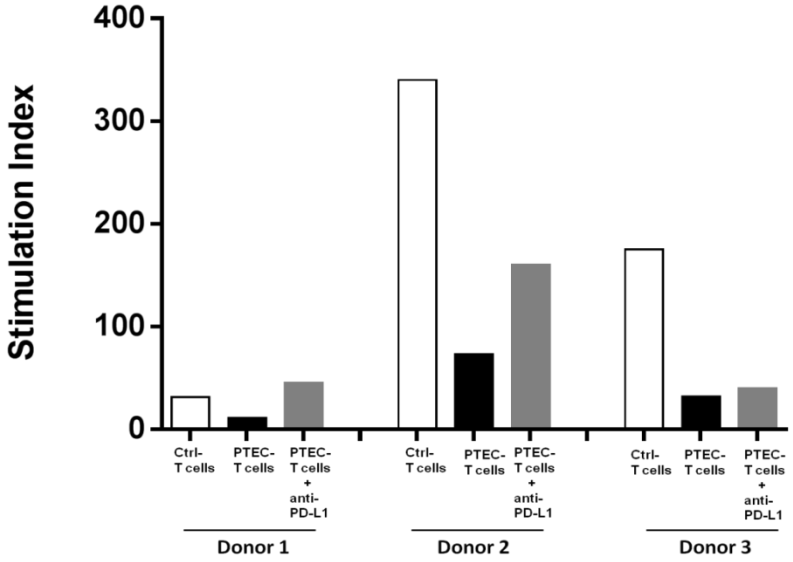

Figure 4.20. PD-L1 partially mediates activated PTEC immune modulation in 3D *in vitro* autologous cultures.

In proliferation experiments performed using 3D cultures; blocking antibody to PD-L1 at 10µg/mL was added to irradiated autologous activated PTEC for 2 hours. Following Ab removal, PTEC were incorporated within collagen gels with purified autologous $CD4^+$ T cells to perform proliferation assays. Figure shows $CD4^+$ T cell responses for 3 separate donors to 40µg/mL phytohaemagglutinin (PHA). White bars represent no PTEC, black bars indicate presence of activated, irradiated (30 Gy) autologous PTEC and grey bars PTEC pre-treated with anti-PD-L1 antibody. Results are expressed as Stimulation index (SI), obtained by dividing means of triplicate test wells by means of relevant triplicate no stimulation control wells.

Further work to investigate the mechanisms by which PTEC down-modulates T cell proliferative responses are being currently undertaken in our laboratory.

4.2.5. Role of IDO in immune modulation of autologous T cells

Research using mouse models has shown that mouse renal epithelial cells are capable of producing the intracellular enzyme indoleamine 2, 3-dioxygenase (IDO) in response to the inflammatory cytokines IFN-γ / TNF-α [65]. Previous studies reported there is a co-relation between IDO expression and Chronic Kidney Disease [66]. IDO is a tryptophan–catabolising enzyme and has immune suppressive effects on T cell functions [46].

Our own unpublished results from the laboratory have demonstrated a partial role for this molecule in immune-modulation in 2D liquid cultures. An initial experiment was undertaken with a single donor sample to assess the role of IDO within a 2D and 3D culture system. The IDO blocking reagent 1-MT was added to facilitate this. Results (presented in **Figure 4.21**) demonstrated at least a partial role for IDO in our observed immune-modulation and there was an additive recovery of proliferation when both PD-L1 and IDO were blocked in the same culture. Due to limited donor samples towards the end of this project, experiments with IDO blocking were confined to only 2 more donor samples within a 3D culture system. Donor 2 showed a similar response to that observed in

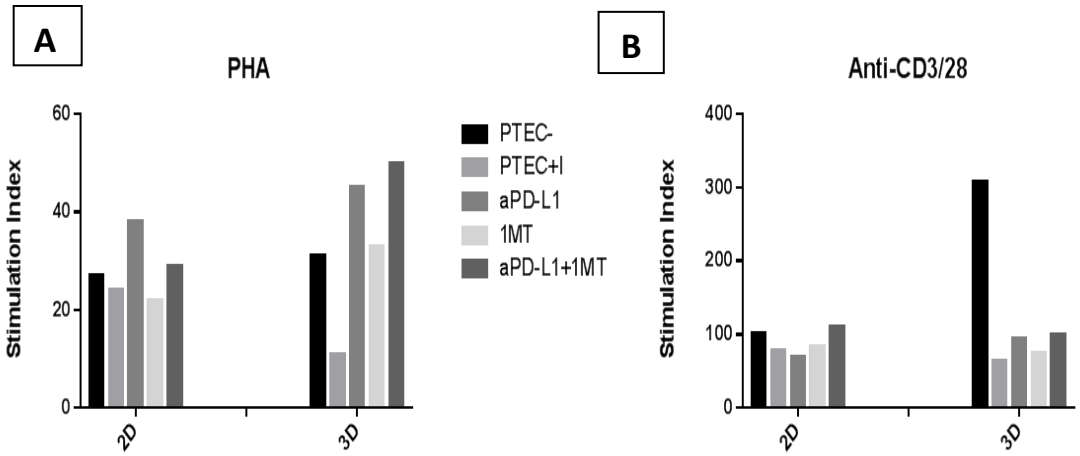

Figure 4.21. Effect of blocking PD-L1 and IDO (using 1MT) on PTEC in 2D and 3D *in vitro* cultures in a representative donor.

Proliferation experiments were performed in 2D (control) and 3D cultures. In 2D and 3D cultures, blocking antibody to PD-L1 was added to irradiated (30 Gy), activated autologous PTEC at 10 µg/mL for 2 h. In 2D cultures, after removal of Ab, $CD4^+$ T cells were added. In 3D cultures, following Ab removal, PTEC were incorporated within collagen gels with purified autologous $CD4^+$ T cells to perform proliferation assays. 1MT at 1500 µM/mL was added to PTEC- T cell co-cultures in 2D and 3D. (A) shows $CD4^+$ T cell responses for one donor to 40 µg/mL phytohaemagglutinin (PHA) (B) T cell responses for the same donor to (0.5/0.1 µg/mL) anti-CD3/CD28. Results are expressed as Stimulation index (SI), obtained by dividing means of triplicate test wells by means of relevant triplicate no stimulation control wells.

Donor 1, with some recovery of proliferation in the presence of blocking to both PD-L1 and IDO (**Figure 4.22 A** and **B**). Whilst Donor 3 demonstrated no recovery in proliferation with blocking of either/both PD-L1 and IDO, possibly due to donor variability/genetics.

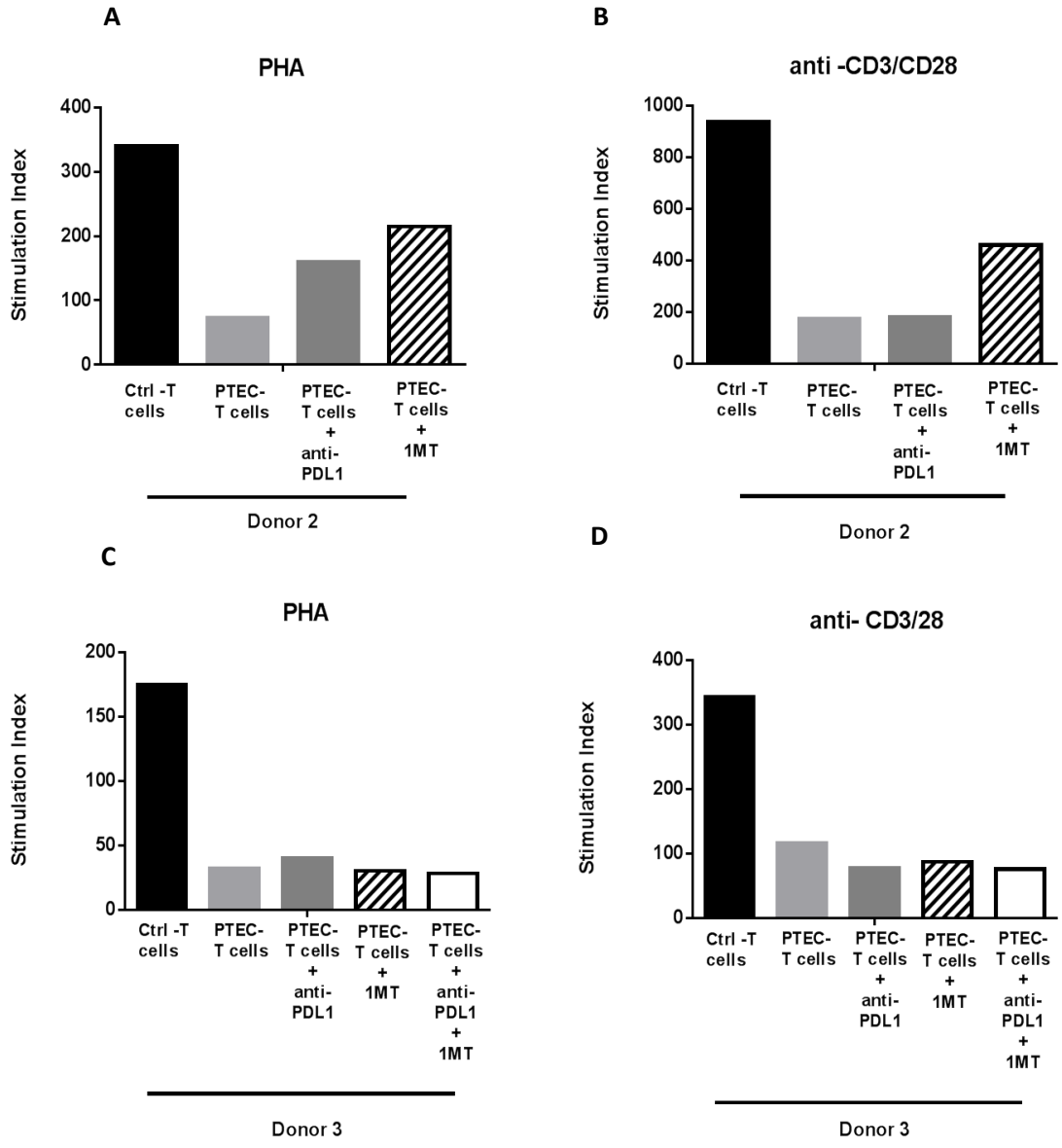

Figure 4.22 Blocking of PTEC with anti-PD-L1 antibody and 1MT in 3D *in vitro* cultures.

Proliferation experiments were performed in 3D *in vitro* cultures. Blocking antibody to PD-L1 was added to irradiated (30 Gy), IFN-γ activated autologous PTEC at 10 µg/mL for 2 h. Following Ab removal, PTEC were incorporated within collagen gels with purified autologous $CD4^+$ T cells to perform proliferation assays. 1MT at 1500 µM/mL was added to PTEC- T cell co-cultures. Figure 4.22 (A) shows $CD4^+$ T cell responses for one donor to 40 µg/mL phytohaemagglutinin (PHA) (B) T cell responses for the same donor to (0.5/0.1 µg/mL) anti-CD3/CD28. (C) and (D) shows the results from a third donor in response to PHA and anti-CD3/CD28 respectively in 3D cultures. Results are expressed as Stimulation Index (SI), obtained by dividing means of triplicate test wells by means of relevant triplicate no stimulation control wells.

4.2.6. Summary

3D *in vitro* cultures enable cells to show appropriate cell responses that closely resemble their native behaviour. In 2D cultures, primary human PTEC cells of the kidney up-regulate surface antigens in response to inflammatory cytokines and are able to down-modulate autologous T cell proliferative responses. Previous blocking studies carried out using 2D cultures confirmed that this down-modulation of immune responses by activated autologous PTEC is partially mediated by PD-L1.

A 3D *in vitro* model to study the PTEC- T cell interactions revealed that under inflammatory disease settings PTEC are capable of up-regulating surface antigen expression. The inflammatory cytokine IFN-γ has a profound effect on the surface expression of PD-L1 and MHC Class II (HLA-DR). TNF-α by itself does not cause any up-regulation of these antigens but can induce a much higher up-regulation of PD-L1 and HLA-DR on PTEC surfaces in conjunction with IFN-γ. In the 3D cultures a higher expression of these antigens was seen compared to the 2D control.

Comparisons of 3D and 2D models revealed enhanced modulation of T cell proliferative responses in 3D compared to 2D. As seen from the results, even within a small sample size, a significant down modulation of T cell proliferative responses was observed in 3D *in vitro* culture. Although a down-modulation in the presence of autologous PTEC in 2D was also seen within this sample size it was not significant, reiterating that 3D cultures allow PTEC to more effectively down modulate immune responses.

PD-L1 is a strong co-inhibitory molecule up-regulated on primary human PTEC under conditions that mimic immunological signalling. The addition of blocking Ab to PD-L1 in 3D and 2D (control) culture systems affirmed that PD-L1 plays a partial role in the down-modulation of T cell proliferation. Another mechanism proposed for inhibition of proliferation by PTEC was by IDO expression. In my cultures, IDO activity was blocked by addition of 1-MT. Results from the 3D cultures demonstrated a partial recovery of inhibition with IDO blockade in two out of three donors. Such donor to donor variability is commonly observed in an out-bred human cohort.

4.3. Chemokines and cytokines produced by PTEC.

4.3.1. Chemokines produced by PTEC

Under diseased conditions, PTEC produce a range of chemokines known to be chemotactic to monocytes, T cells, DC and neutrophils and these chemokines are up-regulated in response to inflammatory mediators like IFN-γ, TGF-β and TNF-α. Using a 2D culture system, the chemokines produced by PTEC in presence of IFN-γ (100 ng/mL) and TGF-β (20 ng/mL) were studied. **Figure 4.23** shows the mean +/- SEM for 4 different donors. Results suggested that within these donors the production of IP-10, MCP-1, MIG and RANTES was induced by IFN-γ. Although TGF-β had minimal effect on chemokine production by itself, a synergistic effect on chemokine synthesis was observed for IP-10, MIG and RANTES when combined with IFN-γ. IL-8 production by PTEC decreased when exposed to IFN- γ. However, more samples are required to be tested to confirm the findings.

Next, the effects of IFN-γ and TNF-α on PTEC were studied as previous results

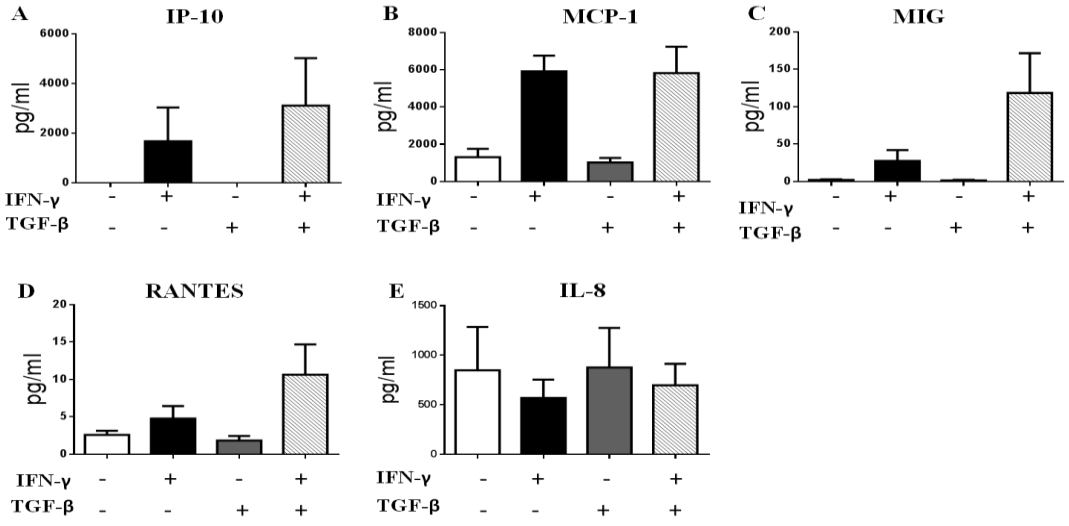

Figure 4.23 Chemokines produced by PTEC in 2D cultures in response to the inflammatory mediators IFN-γ and TGF-β.

PTEC produce a range of chemokines known to be chemotactic to monocytes, T cells, dendritic cells and neutrophils and these chemokines are up-regulated in response to the inflammatory mediators IFN-γ and TGF-β. Data shown are the mean +/- SEM for 4 different donors.

indicated that TGF-β had minimal effect on the chemokine production of PTEC in

2D cultures. To examine the effects of proinflammatory cytokines IFN-γ and TNF-α on chemokine synthesis by PTEC in 3D and 2D cultures, supernatants from the cultures were analysed using a Cytometric Bead Array Human Chemokine kit (BD Biosciences). PTEC were cultured in 96 well plates in duplicates in presence or absence of IFN-γ and TNF-α, or combination of both. For 3D cultures, PTEC were encapsulated within collagen gels and exposed to the pro-inflammatory cytokines. The results in **Figure 4.24** suggested that in the presence of stimulation there was an overall increase in chemokine production both in 2D and 3D cultures. IFN-γ and TNF-α by themselves were able to induce small amounts of RANTES production both in 2D and 3D but an enhanced synthesis of RANTES was observed when these two proinflammatory cytokines were combined. Although IP-10 and MIG synthesis were IFN-γ dependent, the combination of IFN-γ with TNF-α induced the highest level of these two cytokines. IL-8 and MCP-1 were detected in absence of the inflammatory mediators but the levels were up-regulated in the presence of TNF-α and more

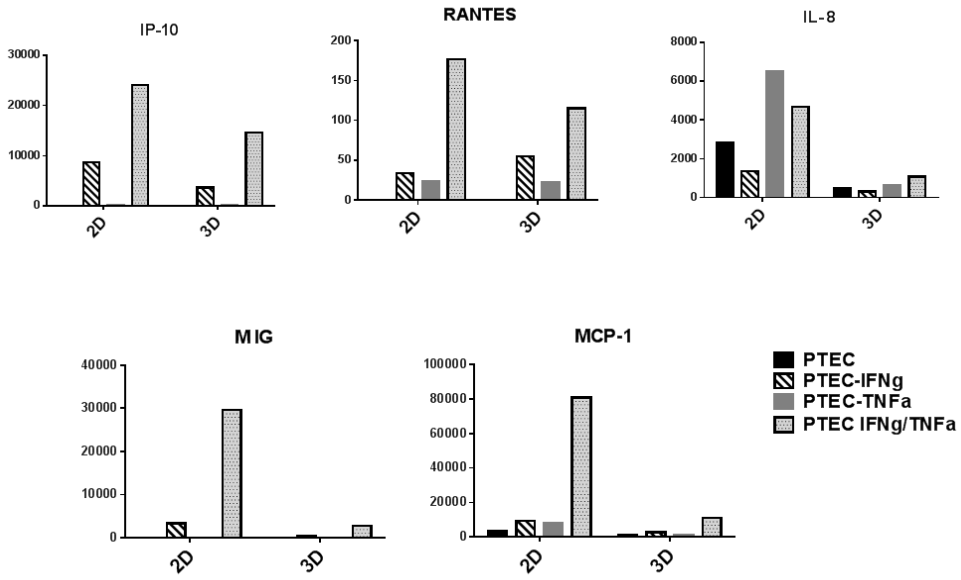

Figure 4.24 Chemokines produced by PTEC in 2D and 3D cultures in response to different inflammatory cytokines. Data derived from a single donor.

PTEC were cultured in 96 well plates in duplicates in presence or absence of IFN-γ, TNF-α or combinations of both in 2D and 3D. In 3D cultures, PTEC were encapsulated within collagen gels and exposed to the pro-inflammatory cytokines. After 36 hours, supernatants were harvested from the cultures and analysed using a Cytometric Bead Array kit.

so in synergy with IFN-γ, especially within 3D cultures. Interestingly, in 3D cultures, levels of chemokines produced by PTEC in response to these

inflammatory cytokines were consistently lower than those in 2D cultures. This preliminary data could possibly reflect the fact that within 3D cultures the cells displayed a less stressed functionality, therefore secreting less chemokines in response to inflammatory stimuli. However, more data is required to confirm the findings.

PTEC were also analysed alone in both 2D and 3D cultures and found not to produce IL-10, IL-12p70 and IL-1β (data not shown).

4.3.2. Immune–cell cytokine profiles in the presence of autologous PTEC in 3D collagen model.

Cytokine profiles from $CD4^+$ T cells in the presence of autologous PTEC were analysed from supernatants of 2D cultures (Donor 1) using Cytometric Bead Array (CBA) Human T_h1/T_h2 Cytokine Kit II (BD Biosciences). As seen in **Figure 4.25** a decrease in the amounts of IFN-γ, IL-10 and IL-2 was detected in presence of PTEC when T cells were stimulated with anti-CD3/CD28. Optimal stimulation was observed through the TCR with anti-CD3/28 inducing the highest expression of all cytokines. With PHA stimulation of T cells, a slight increase in IFN-γ and IL-10 levels were noted. Also, concurrently sharp increases in IL-4 levels were observed in the supernatants. These results suggest that the presence of PTEC causes a decrease in Th1 type cytokines while enhancing the production of Th2 type cytokines (IL-4). TNF-α synthesis decreased in presence of PTEC when T cells were stimulated with anti-CD3/28. IL-6 production was not monitored because PTEC alone produce higher levels of this cytokine than that produced by T cells.

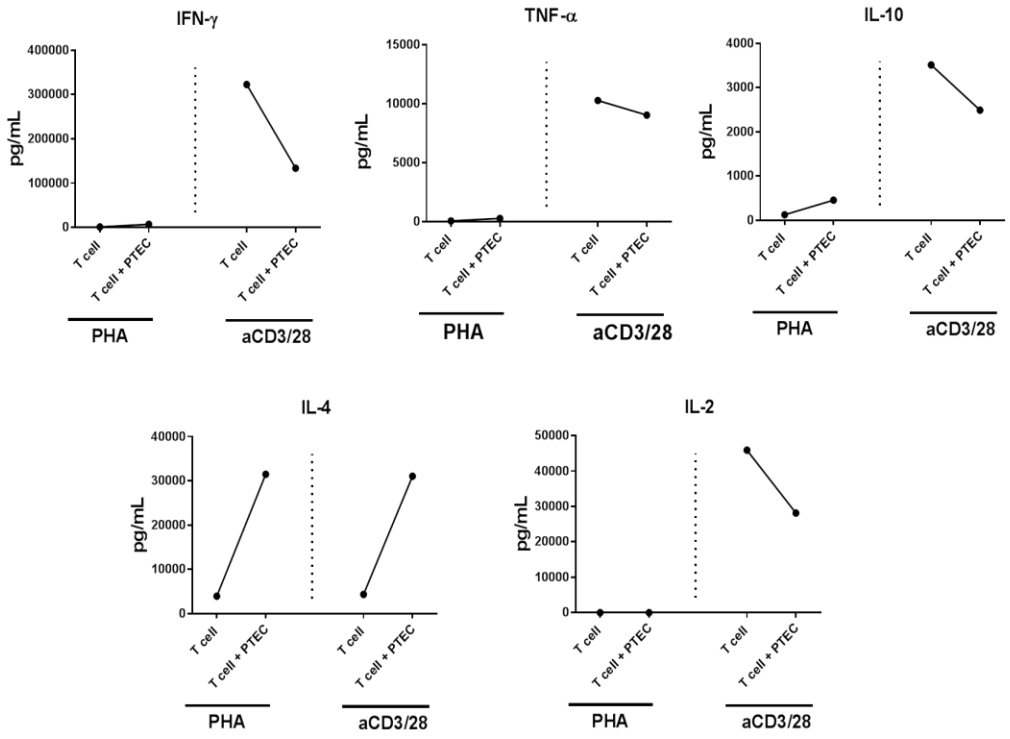

Figure 4.25 Cytokine profiles of responding CD4$^+$ T cells in presence of activated autologous PTEC (Donor 1) in 2D cultures.

Supernatants from 2D cultures of autologous CD4$^+$ T cells and PTEC were harvested after 36 h in culture and analysed using Cytometric Bead Array (CBA) Human Th1/Th2 Cytokine Kit II (BD Biosciences).

Following this, another donor was selected and the supernatants from proliferation assays in 2D and 3D cultures were tested to detect Th1/Th2 type cytokines present. Decreases in IFN-γ, IL-2, TNF, and an increase in IL-4 were detected in the 3D model. The pattern of expression of cytokines in the presence of PTEC for donor 2 was similar to that of donor 1 both in 2D and 3D for all the cytokines except IL-4. In the 3D *in vitro* culture, the IL-4 mirrored the results from donor 1 but in the 2D culture IL-4 increased in the presence of PTEC (**Figure 4.26).** The results indicated that in the presence of PTEC there was a skewing of cytokines from a Th1 towards a Th2 type profile in 2D and 3D *in vitro* cultures.

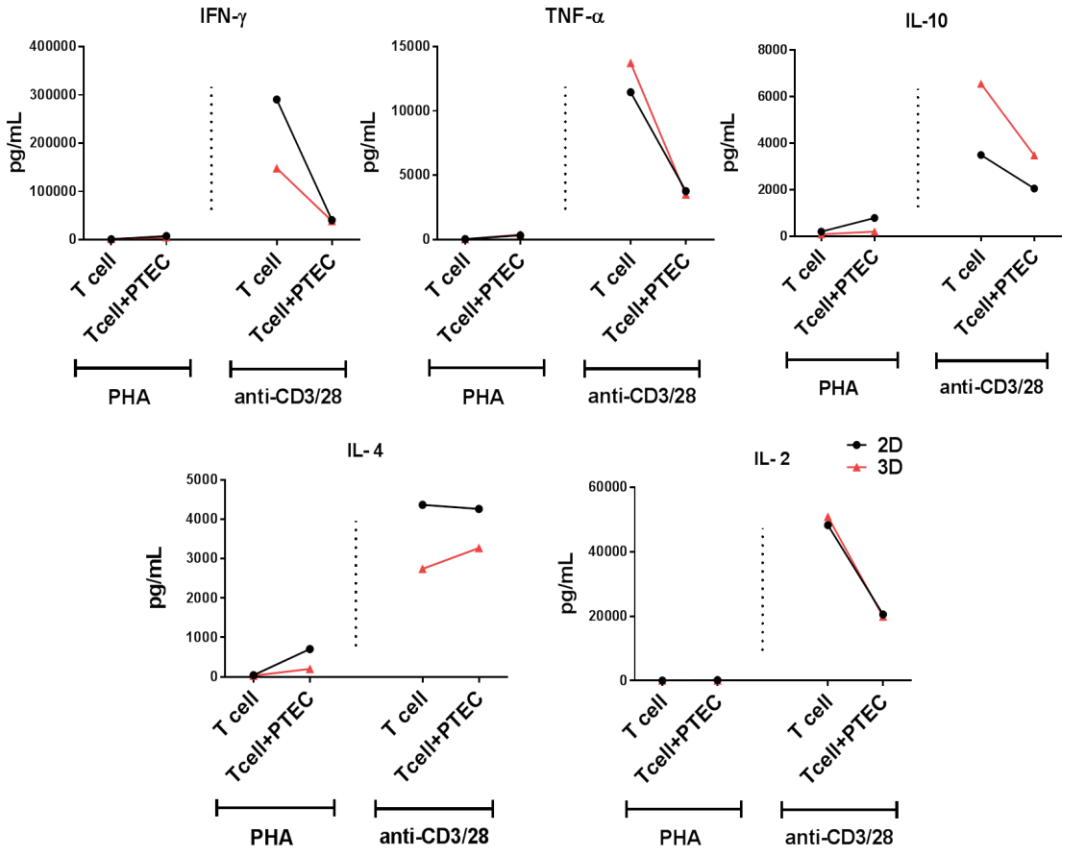

Figure 4.26 Cytokines produced in presence of activated autologous PTEC (Donor 2) in 2D and 3D *in vitro* cultres.

Supernatants from proliferation assays in 2D and 3D cultures were harvested at 36 h and tested to detect the pattern of expression of cytokines using Cytometric Bead Array (CBA) Human Th1/Th2 Cytokine Kit II (BD Biosciences).

4.3.3. Summary

Under diseased conditions, PTEC produce a range of chemokines known to be chemotactic to monocytes, T cells, DC and neutrophils and these chemokines are up-regulated in response to inflammatory mediators like IFN-γ, TGF-β and TNF-α. Once these cells are recruited, they can promote further chemokine production from the PTEC. In this thesis, the influence of a more *in vivo* like 3D model on the chemokines and cytokines produced by primary human PTEC in presence of pro-inflammatory cytokines was explored.

When exposed to IFN-γ or TGF-β and a combination of both, the production of IP-10, MCP-1, MIG and RANTES was induced by IFN-γ only. Although TGF-β did not have much effect on chemokine production by itself, it provided a synergistic effect on chemokine synthesis for IP-10, MIG and RANTES when combined with IFN-γ. IL-8 production by PTEC decreased when exposed to IFN-γ.

In the presence of IFN-γ and TNF-α, there was an overall increase in chemokine production, both in 2D and 3D cultures. Interestingly, within this sample, the levels of chemokines produced by PTEC in 3D cultures in response to inflammatory cytokines IFN-γ and TNF-α and both together, were consistently lower than 2D cultures perhaps indicating that cells in 3D cultures were less stressed. There is also a possibility that the cytokines were bound to the collagen matrix and were therefore seemingly lower in abundance in the supernatants compared to 2D.The results from the Th1/Th2 cytokine detection kit indicated that in presence of PTEC the cytokines produced by responding T cells cause a skewing of cytokines from Th1 towards Th2 type profile in 2D and 3D *in vitro* cultures.

Chapter 5: Discussion and conclusions

5.1. Discussion

This thesis aimed to develop a 3D hydrogel system for the co-culture of PTEC and immune cells. To construct a versatile model, various types of hydrogels were investigated. Besides establishing a suitable biomaterial that would closely resemble the native ECM, the thesis also focused on identifying techniques of recovering the cells from the gel matrix to analyse their phenotypic and functional characteristics. The immunomodulatory functions of the recovered cells were examined and compared with the results from 2D cultures.

It is known that in the early stages of kidney disease PTEC play an important role in bringing in inflammatory immune cells into the kidney interstitium and are capable of modulating the functions of these immune cells. In 2011, Wilkinson *et al* were able to demonstrate, for the first time, that primary human PTEC can modulate autologous T cell and B cell and DC responses [3, 45]. All these studies were carried out in traditional 2D cultures. Research has provided evidence that culture conditions affect cell physiology profoundly [125]. I hypothesized that a 3D model that better mimic physiological conditions would allow the kidney cells and immune cells to exhibit their typical phenotype and functionality and this may provide new and interesting insights in regards to how these cells interact with each other under *in vivo* conditions.

In this study various hydrogels and hydrogel mixtures were used to obtain a suitable matrix. The mechanical properties of hydrogels are important for adhesion of cells and the expression of various genes. Adhesion, migration or differentiation of cells are significantly affected by the interactions of the cells with the hydrogels that form the ECM [126]. Alginate gels to some extent are similar to ECM in tissues but lack cell adhesion sites and allow no interaction between the gel and the cells [89]. For PTEC and T cells, the alginate gels allowed a homogenous cell distribution within the hydrogel but cell viability was low, limiting its use in creating engineered tissue. To enhance the chances of cell binding and spreading within the gel, cell binding motifs were introduced by

mixing alginate with either collagen or Matrigel. Though it improved cell viability within the gel mixtures compared to alginate itself, considerable numbers of cells still died within a week of culture making it unsuitable for the *in vitro* model.

Next, photopolymerizable GelMA hydrogel was studied as a potential ECM for PTEC and T cell co-culture. The advantages of GelMA are that it is derived from inexpensive gelatin and is comprised of modified natural ECM components [127]. Gelatin has a wide use in tissue engineering applications and has been successfully used to culture different cell types like immortalized HUVEC, NIH 3T3 fibroblasts [108] and aortic VICs [112]. PTEC readily bound, spread and formed interconnections on GelMA, demonstrating the ability of the gel to sustain viable PTEC for at least 4 weeks. PTEC formed networks after weeks in culture. The short UV exposure of $CD4^+$ T cells during the encapsulation process in GelMA did not affect viability of T cells although live cell imaging provided evidence that T cells were incapable of migrating within GelMA and viability of T cells decreased over time. No significant movement of T cells within GelMA was observed, perhaps due to the inability of T cells to degrade and remodel the matrix. The possibility of T cell death due to continuous exposure to laser light was excluded as the microscope (Cell Voyager CV1000) used to take the time lapse images is a spinning disk confocal microscope which uses microlens enhanced dual Nipkow disk scanning technology and has drastically reduced phototoxicity and photobleaching [128]. Only a low level of laser power at the specimen is required to fully excite fluorescence. Moreover, the time lapse images of the cells within the collagen gel were captured using this same scanning disk confocal and the same settings. As shown in the results, the cells migrated through the collagen gels with ease. Overall the results suggested that GelMA was not well suited for co-culture of PTEC and T cells.

Collagen fibres are one of the main components of the tissue stroma through which lymphocytes migrate *in vivo* [102]. Collagen gels have been used to study migrations of highly motile T cells [106]. The kidney cell line MDCK has also been cultured and studied in collagen gels [107]. Thus this thesis also investigated the suitability of a collagen type I gel model. Within the collagen gel model system, T cell migration and PTEC movement was observed using live-cell phase contrast and fluorescence microscopy. Time lapse video microscopy demonstrated

dynamic cell – cell interactions suggesting that the collagen gel model system provided a suitable ECM for cell co-culture.

Single cells tracked within this gel system using Image J software revealed that the presence of PTEC slowed down movement of T cells within the gel due to the interactions between the cell types. These interactions arrested the movement of the T cells. The T cells migrated away from the PTEC after the interaction. Such contact "dwell times" are known to be important in a number of immune cell modulation/activation events including those that occur at the immune-synapse between DC and T cells [129].

Earlier study on primary human PTEC in 2D culture showed that IFN-γ had the most profound effect on up-regulation of PD-L1 and MHC II (HLA-DR) expression [3]. Consistent with that study, PTEC in our 3D *in vitro* model also showed upregulation of PD-L1 and HLA-DR when treated with IFN-γ. Research with murine models of kidney diseases have shown that TNF-α plays a role in inflammatory renal diseases [130]. There is evidence that the presence of TNF-α in inflamed human kidneys is positively associated with the risk of developing CKD [131]. Thus, in this study, PTEC were also treated with TNF-α and a combination of both IFN-γ and TNF-α. The synergistic effect of the two proinflammatory cytokines were observed in 2 donor samples inducing a maximum level of PD-L1 and MHC II expression on the PTEC both in 2D and 3D cultures. However, the data obtained suggested that a higher expression of these surface Ags occurred in the 3D model compared to 2D.

The proliferative responses of $CD4^+$ T cells in presence of autologous PTEC under inflammatory conditions were studied in 2D and 3D models. In the presence of activated autologous PTEC, inhibition of T cell proliferative responses was observed in 2D and 3D cultures. However, this down-modulation was seen to be greater in 3D cultures than in 2D cultures. One mechanistic explanation for this could be that PTEC within 3D cultures displayed a greater level of HLA-DR and PD-L1, enabling them to interact with PD-1 and down-modulate $CD4^+$ T cells more effectively. This inhibition was seen when T cells were stimulated via their TCR complex using anti-CD3/28 Ab or through mitogenic stimulation with PHA. Proliferative responses of T cells were down modulated in 5 of 6 donors when stimulated with PHA. Also the proliferative

responses varied between donors. These differences are commonly seen in out-bred human samples. Thus the results indicated that the 3D culture model was a more effective system compared to the conventional 2D culture and enabled the cells to show appropriate cell physiological responses. Other factors apart from increased levels of surface antigen expression may also contribute to the more effective 3D culture system. In the 3D system, the PTEC were more widely distributed within the hydrogel and T cells were able to successfully move through the gel having more contact with the PTEC cells. In contrast, in the 2D culture system PTEC formed a monolayer and therefore only a fraction of their cell surfaces were exposed to the T cells in culture.

PTEC express and produce multiple molecules which enable them to function as immunomodulatory cells. From previous research it is known that activated PTEC act as non-professional APC and down-regulate autologous T cell and B cell proliferative responses in 2D cultures and this modulation is partially mediated by PD-L1. Here in this thesis, blocking Ab to PD-L1 was used in 3D cultures to confirm that this molecule also plays a role in immune modulation within this more representative *in vivo* culture system. The modulation by PTEC involves complex mechanisms and multiple molecules. The role of IDO expression by primary human PTEC and its effect on autologous T cell proliferation was evaluated in 3D cultures. Out of 3 donors, addition of 1-MT (inhibitor of IDO) resulted in partial amelioration of inhibition in 2 donors in 3D. Within the scope and timeline of this thesis, there were not enough suitable donors to repeat this study and further confirm the role of IDO in 3D cultures.

Aggregation of T cells occurs in the kidney interstitium in many renal diseases but the mechanisms by which the T cells cause interstitial injury are not well characterized. Research has demonstrated that this interstitial infiltration of cells is directed by chemokines released by damaged or activated PTEC [24, 25].

In this thesis the effect of proinflammatory cytokines IFN-γ, TNF-α and combinations of both on PTEC in 3D cultures were studied. Our previous published paper with 2D cultures demonstrated that the cytokine profile shifted away from the Th1 type profile towards a Th2 type profile [3]. This study confirmed that within 3D *in vitro* cultures, higher levels of IL-4 and lower levels of IFN-γ, TNF-α, IL-2 and IL-10 were also produced in the presence of activated

autologous PTEC, emphasizing that these cells induce a shift away from an inflammatory Th1 responder T cell profile towards a Th2 type profile in the 3D *in vitro* model. Highest levels of cytokines were expressed when $CD4^+$ T cell stimulation occurred through their TCR complex using anti-CD3/28.

5.2. Conclusions and Future directions

In conclusion, it was evident from the results that a 3D *in vitro* model of collagen was well suited to co-culture PTEC and T cells. As using this 3D collagen matrix model, we could easily observe migration of T cells and their interactions with PTEC under *in vivo*-like inflammatory conditions using time lapse video microscopy. In addition, PTEC were able to down-modulate T cell immune responses more effectively within this collagen based model as opposed to their 2D controls. Collagen gels could be dissolved easily to recover the cells and study their expression of cell surface antigens. Consistent with 2D cultures, activated PTEC were capable of up-regulating PD-L1 and MHC class II molecules within this 3D *in vitro* model. Also $CD4^+$ T cells up-regulated their activation markers within the collagen gels. The cytokine profiles of responding $CD4^+$ T cells in the presence of activated autologous PTEC in the 3D *in vitro* model were consistent with 2D results and suggested that the cytokine profile resembled more the Th2 type.

Overall the results suggested that the 3D *in vitro* model created an environment where both cell types expressed a more *in vivo* like phenotype. PTEC were capable of showing a greater down-modulation of proliferative responses of the $CD4^+$ T cells within the 3D collagen model as compared to the 2D culture system.

An interesting observation in the time lapse videos of PTEC (refer video 3) cultured in collagen revealed small vesicle-like structures being released by these cells. There could be the possibility that such vesicles contain a range of factors or molecules that could be involved in our observed immune modulation. However it should also be noted that apoptotic cells undergo blebbing which may partially account for what we have observed in the videos. Further characterization is needed to draw any conclusions.

Further investigation of the mechanisms by which PTEC modulate the autologous immune responses using the 3D collagen model may reveal new interesting insights and enhance our understanding of the role of PTEC during inflammatory kidney disease. This may enable us to offer targets for diagnostic and therapeutic intervention at earlier stages of renal disease.

Bibliography

1. Zhang, G., *Projections of the incidence of treated end-stage kidney disease in Australia, 2010-2020. Cat. no. PHE 150. Canberra: AIHW.* 2011.
2. Graf, J., F. Green, and C. Ryan, *An Overview of Chronic Kidney Disease in Australia 2009*. 2009: Australian Institute of Health and Welfare.
3. Wilkinson, R., et al., *Activated human renal tubular cells inhibit autologous immune responses.* Nephrol Dial Transplant, 2011. **26**(5): p. 1483-92.
4. Lutolf, M.P., P.M. Gilbert, and H.M. Blau, *Designing materials to direct stem-cell fate.* Nature, 2009. **462**(7272): p. 433-441.
5. Lelongt, B. and P. Ronco, *Role of extracellular matrix in kidney development and repair.* Pediatric Nephrology, 2003. **18**(8): p. 731-742.
6. Klein, T.J., et al., *Long-term effects of hydrogel properties on human chondrocyte behavior.* Soft Matter, 2010. **6**(20): p. 5175-5183.
7. Bott, K., et al., *The effect of matrix characteristics on fibroblast proliferation in 3D gels.* Biomaterials, 2010. **31**(32): p. 8454-64.
8. Eric P. Widmaier, Hershel Raff, and K.T. Strang., *The Kidney and Regulation of Water and Inorganic Ions*, in *Vander's Human Physiology: The Mechanisms of Body Function*. 2006, McGraw-Hill: New York.
9. Kurts, C., et al., *The immune system and kidney disease: basic concepts and clinical implications.* Nature Reviews Immunology, 2013. **13**(10): p. 738-753.
10. Marshall, R.J. and A.G. MacIver, *The monocyte/macrophage population of the normal human kidney.* J Pathol, 1984. **143**(4): p. 275-80.
11. Segerer, S., et al., *Compartment specific expression of dendritic cell markers in human glomerulonephritis.* Kidney International, 2008. **74**(1): p. 37-46.
12. Dankers, P.Y.W., et al., *From kidney development to drug delivery and tissue engineering strategies in renal regenerative medicine.* Journal of Controlled Release, 2011. **152**(1): p. 177-185.
13. Geiger, B., et al., *Transmembrane crosstalk between the extracellular matrix and the cytoskeleton.* Nat Rev Mol Cell Biol, 2001. **2**(11): p. 793-805.
14. Grygielko, E.T., et al., *Inhibition of gene markers of fibrosis with a novel inhibitor of transforming growth factor-beta type I receptor kinase in puromycin-induced nephritis.* J Pharmacol Exp Ther, 2005. **313**(3): p. 943-51.
15. Caldas, H.C., A.P.C. Hayashi, and M. Abbud-Filho, *Repairing the Chronic Damaged Kidney: The Role of Regenerative Medicine.* Transplantation Proceedings, 2011. **43**(10): p. 3573-3576.
16. Daha, M.R. and C. van Kooten, *Is the proximal tubular cell a proinflammatory cell?* Nephrology Dialysis Transplantation, 2000. **15**(suppl 6): p. 41-43.
17. Kriz, W., N. Gretz, and K.V. Lemley, *Progression of glomerular diseases: Is the podocyte the culprit?* Kidney Int, 1998. **54**(3): p. 687-697.
18. Risdon, R.A., J.C. Sloper, and H.E. De Wardener, *Relationship between renal function and histological changes found in renal-biopsy specimens from patients with persistent glomerular nephritis.* Lancet, 1968. **2**(7564): p. 363-6.

19. Cameron, J.S., *Clinicopathologic Correlations in Glomerular Disease*, in *Kidney Disease: Present status*. 1970. p. 81-84.
20. Hostetter, T.H., et al., *Hyperfiltration in remnant nephrons: a potentially adverse response to renal ablation.* Am J Physiol, 1981. **241**(1): p. F85-93.
21. Bertani, T., et al., *Tubulo-interstitial lesions mediate renal damage in adriamycin glomerulopathy.* Kidney Int, 1986. **30**(4): p. 488-96.
22. Remuzzi, G., A. Benigni, and A. Remuzzi, *Mechanisms of progression and regression of renal lesions of chronic nephropathies and diabetes.* J Clin Invest, 2006. **116**(2): p. 288-96.
23. Ziyadeh, F.N., et al., *High glucose induces cell hypertrophy and stimulates collagen gene transcription in proximal tubule.* Am J Physiol, 1990. **259**(4 Pt 2): p. F704-14.
24. Zoja, C., et al., *Protein overload stimulates RANTES production by proximal tubular cells depending on NF-kappa B activation.* Kidney Int, 1998. **53**(6): p. 1608-15.
25. Lai, K.N., et al., *Interaction between proximal tubular epithelial cells and infiltrating monocytes/T cells in the proteinuric state.* Kidney Int, 2007. **71**(6): p. 526-38.
26. Gerritsma, J., et al., *Regulation and production of IL-8 by human proximal tubular epithelial cells in vitro.* Clinical & Experimental Immunology, 1996. **103**(2): p. 289-294.
27. Hart, D.N. and J.W. Fabre, *Endogenously produced Ia antigens within cells of convoluted tubules of rat kidney.* J Immunol, 1981. **126**(6): p. 2109-13.
28. van Kooten, C., et al., *Possible role for CD40-CD40L in the regulation of interstitial infiltration in the kidney.* Kidney Int, 1997. **51**(3): p. 711-21.
29. Hutloff, A., et al., *ICOS is an inducible T-cell co-stimulator structurally and functionally related to CD28.* Nature, 1999. **397**(6716): p. 263-6.
30. Freeman, G.J., et al., *Engagement of the Pd-1 Immunoinhibitory Receptor by a Novel B7 Family Member Leads to Negative Regulation of Lymphocyte Activation.* The Journal of Experimental Medicine, 2000. **192**(7): p. 1027-1034.
31. Rubin-Kelley, V. and A.M. Jevnikar, *Antigen presentation by renal tubular epithelial cells.* Journal of the American Society of Nephrology, 1991. **2**(1): p. 13-26.
32. Ting, J.P. and J. Trowsdale, *Genetic control of MHC class II expression.* Cell, 2002. **109 Suppl**: p. S21-33.
33. Greenwald, R.J., Y.E. Latchman, and A.H. Sharpe, *Negative co-receptors on lymphocytes.* Current opinion in immunology, 2002. **14**(3): p. 391-396.
34. Schoop, R., et al., *Suppressed T-cell activation by IFN-gamma-induced expression of PD-L1 on renal tubular epithelial cells.* Nephrol Dial Transplant, 2004. **19**(11): p. 2713-20.
35. Ding, H., X. Wu, and W. Gao, *PD-L1 is expressed by human renal tubular epithelial cells and suppresses T cell cytokine synthesis.* Clinical Immunology, 2005. **115**(2): p. 184-191.
36. Hagerty, D. and P. Allen, *Processing and presentation of self and foreign antigens by the renal proximal tubule.* The Journal of Immunology, 1992. **148**(8): p. 2324-2330.
37. Dong, H., et al., *Tumor-associated B7-H1 promotes T-cell apoptosis: a potential mechanism of immune evasion.* Nature medicine, 2002. **8**(8): p. 793-800.

38. Mazanet, M.M. and C.C. Hughes, *B7-H1 is expressed by human endothelial cells and suppresses T cell cytokine synthesis.* The Journal of Immunology, 2002. **169**(7): p. 3581-3588.
39. Blank, C. and A. Mackensen, *Contribution of the PD-L1/PD-1 pathway to T-cell exhaustion: an update on implications for chronic infections and tumor evasion.* Cancer immunology, immunotherapy, 2007. **56**(5): p. 739-745.
40. Schoop, R., et al., *Suppressed T-cell activation by IFN-{gamma}-induced expression of PD-L1 on renal tubular epithelial cells.* Nephrol. Dial. Transplant., 2004. **19**(11): p. 2713-2720.
41. de Haij, S., et al., *Renal tubular epithelial cells modulate T-cell responses via ICOS-L and B7-H1.* Kidney Int, 2005. **68**(5): p. 2091-2102.
42. Waeckerle-Men, Y., A. Starke, and R.P. Wuthrich, *PD-L1 partially protects renal tubular epithelial cells from the attack of CD8+ cytotoxic T cells.* Nephrol Dial Transplant, 2007. **22**(6): p. 1527-36.
43. Starke, A., et al., *Renal tubular PD-L1 (CD274) suppresses alloreactive human T-cell responses.* Kidney Int, 2010. **78**(1): p. 38-47.
44. Chen, Y., et al., *Expression of B7-H1 in inflammatory renal tubular epithelial cells.* Nephron Exp Nephrol, 2006. **102**(3-4): p. e81-92.
45. Kassianos, A.J., et al., *Human proximal tubule epithelial cells modulate autologous dendritic cell function.* Nephrology Dialysis Transplantation, 2013. **28**(2): p. 303-312.
46. Godin-Ethier, J., et al., *Human activated T lymphocytes modulate IDO expression in tumors through Th1/Th2 balance.* J Immunol, 2009. **183**(12): p. 7752-60.
47. Löb, S., et al., *Inhibitors of indoleamine-2, 3-dioxygenase for cancer therapy: can we see the wood for the trees?* Nature Reviews Cancer, 2009. **9**(6): p. 445-452.
48. Lee, G.K., et al., *Tryptophan deprivation sensitizes activated T cells to apoptosis prior to cell division.* Immunology, 2002. **107**(4): p. 452-460.
49. Munn, D.H., et al., *Prevention of allogeneic fetal rejection by tryptophan catabolism.* Science, 1998. **281**(5380): p. 1191-1193.
50. Kudo, Y. and C. Boyd, *Human placental indoleamine 2, 3-dioxygenase: cellular localization and characterization of an enzyme preventing fetal rejection.* Biochimica et Biophysica Acta (BBA)-Molecular Basis of Disease, 2000. **1500**(1): p. 119-124.
51. Kwidzinski, E. and I. Bechmann, *IDO expression in the brain: a double-edged sword.* Journal of Molecular Medicine, 2007. **85**(12): p. 1351-1359.
52. Guillemin, G.J., et al., *Expression of indoleamine 2, 3-dioxygenase and production of quinolinic acid by human microglia, astrocytes, and neurons.* Glia, 2005. **49**(1): p. 15-23.
53. Ohtaki, H., et al., *Kynurenine production mediated by indoleamine 2,3-dioxygenase aggravates liver injury in HBV-specific CTL-induced fulminant hepatitis.* Biochim Biophys Acta, 2014.
54. Kiank, C., et al., *Psychological stress-induced, IDO1-dependent tryptophan catabolism: implications on immunosuppression in mice and humans.* PLoS One, 2010. **5**(7): p. e11825.
55. Jalili, R.B., et al., *Suppression of islet allogeneic immune response by indoleamine 2,3 dioxygenase-expressing fibroblasts.* J Cell Physiol, 2007. **213**(1): p. 137-43.

56. Lahdou, I., et al., *Role of human corneal endothelial cells in T-cell mediated allo-immune attack in vitro.* Investigative ophthalmology & visual science, 2013: p. IOVS-13-11930.
57. Meisel, R., et al., *Human bone marrow stromal cells inhibit allogeneic T-cell responses by indoleamine 2, 3-dioxygenase–mediated tryptophan degradation.* Blood, 2004. **103**(12): p. 4619-4621.
58. Uyttenhove, C., et al., *Evidence for a tumoral immune resistance mechanism based on tryptophan degradation by indoleamine 2, 3-dioxygenase.* Nature medicine, 2003. **9**(10): p. 1269-1274.
59. Brandacher, G., et al., *Prognostic value of indoleamine 2, 3-dioxygenase expression in colorectal cancer: effect on tumor-infiltrating T cells.* Clinical Cancer Research, 2006. **12**(4): p. 1144-1151.
60. Munn, D.H., et al., *Inhibition of T cell proliferation by macrophage tryptophan catabolism.* The Journal of experimental medicine, 1999. **189**(9): p. 1363-1372.
61. Hwu, P., et al., *Indoleamine 2, 3-dioxygenase production by human dendritic cells results in the inhibition of T cell proliferation.* The Journal of Immunology, 2000. **164**(7): p. 3596-3599.
62. Taylor, M. and G. Feng, *Relationship between interferon-gamma, indoleamine 2, 3-dioxygenase, and tryptophan catabolism.* The FASEB Journal, 1991. **5**(11): p. 2516-2522.
63. Robinson, C.M., P.T. Hale, and J.M. Carlin, *The role of IFN-γ and TNF-α-responsive regulatory elements in the synergistic induction of indoleamine dioxygenase.* Journal of interferon & cytokine research, 2005. **25**(1): p. 20-30.
64. Arioka, Y., et al., *Pre-administration of L-tryptophan improved ADR-induced early renal failure in mice.* Life sciences, 2012. **91**(3): p. 100-106.
65. Mohib, K., et al., *Proapoptotic activity of indoleamine 2, 3-dioxygenase expressed in renal tubular epithelial cells.* American Journal of Physiology-Renal Physiology, 2007. **293**(3): p. F801-F812.
66. Schefold, J.C., et al., *Increased indoleamine 2, 3-dioxygenase (IDO) activity and elevated serum levels of tryptophan catabolites in patients with chronic kidney disease: a possible link between chronic inflammation and uraemic symptoms.* Nephrology Dialysis Transplantation, 2009. **24**(6): p. 1901-1908.
67. Alberts B, J.A., Lewis J, et al. Molecular Biology of the Cell. 4th edition. New York: Garland Science; 2002. *Lymphocytes and the Cellular Basis of Adaptive Immunity*. Available from: http://www.ncbi.nlm.nih.gov/books/NBK26921/, *Lymphocytes and the Cellular Basis of Adaptive Immunity*. 2002. **4th edition**.
68. Mempel, T.R., S.E. Henrickson, and U.H. von Andrian, *T-cell priming by dendriticcells in lymph nodes occurs in three distinct phases.* Nature, 2004. **427**(6970): p. 154-159.
69. Bettelli, E., T. Korn, and V.K. Kuchroo, *Th17: the third member of the effector T cell trilogy.* Current opinion in immunology, 2007. **19**(6): p. 652-657.
70. Singer, G.G., et al., *Stimulated renal tubular epithelial cells induce anergy in CD4^+ T cells.* Kidney international, 1993. **44**: p. 1030-1030.
71. Kuroiwa, T., et al., *Distinct T Cell/Renal Tubular Epithelial Cell Interactions Define Differential Chemokine Production: Implications for Tubulointerstitial Injury in Chronic Glomerulonephritides.* The Journal of Immunology, 2000. **164**(6): p. 3323-3329.

72. Segerer, S., et al., *CXCR3 is involved in tubulointerstitial injury in human glomerulonephritis.* The American journal of pathology, 2004. **164**(2): p. 635-649.
73. Freeman, G.J., et al., *Engagement of the PD-1 immunoinhibitory receptor by a novel B7 family member leads to negative regulation of lymphocyte activation.* The Journal of experimental medicine, 2000. **192**(7): p. 1027-1034.
74. Rot, A. and U.H. von Andrian, *Chemokines in innate and adaptive host defense: basic chemokinese grammar for immune cells.* Annu. Rev. Immunol., 2004. **22**: p. 891-928.
75. Murphy, P.M., *International Union of Pharmacology. XXX. Update on chemokine receptor nomenclature.* Pharmacological reviews, 2002. **54**(2): p. 227-229.
76. Middleton, J., et al., *Leukocyte extravasation: chemokine transport and presentation by the endothelium.* Blood, 2002. **100**(12): p. 3853-3860.
77. Segerer, S., P.J. Nelson, and D. SCHLÖNDORFF, *Chemokines, chemokine receptors, and renal disease: from basic science to pathophysiologic and therapeutic studies.* Journal of the American Society of Nephrology, 2000. **11**(1): p. 152-176.
78. Banas, B., et al., *Binding of the chemokine SLC/CCL21 to its receptor CCR7 increases adhesive properties of human mesangial cells.* Kidney international, 2004. **66**(6): p. 2256-2263.
79. Esche, C., C. Stellato, and L.A. Beck, *Chemokines: Key Players in Innate and Adaptive Immunity.* J Investig Dermatol, 2005. **125**(4): p. 615-628.
80. Anders, H.-J., V. Vielhauer, and D. Schlöndorff, *Chemokines and chemokine receptors are involved in the resolution or progression of renal disease.* Kidney international, 2003. **63**(2): p. 401-415.
81. Chakravorty, S.J., et al., *Fractalkine expression on human renal tubular epithelial cells: potential role in mononuclear cell adhesion.* Clinical & Experimental Immunology, 2002. **129**(1): p. 150-159.
82. Cockwell, P., et al., *Chemoattraction of T cells expressing CCR5, CXCR3 and CX3CR1 by proximal tubular epithelial cell chemokines.* Nephrology Dialysis Transplantation, 2002. **17**(5): p. 734-744.
83. Demmers, M.W., et al., *Differential effects of activated human renal epithelial cells on T-cell migration.* PloS one, 2013. **8**(5): p. e64916.
84. Holt, D.J., L.M. Chamberlain, and D.W. Grainger, *Cell-cell signaling in co-cultures of macrophages and fibroblasts.* Biomaterials, 2010. **31**(36): p. 9382-94.
85. Chamberlain, L.M., et al., *Phenotypic non-equivalence of murine (monocyte-) macrophage cells in biomaterial and inflammatory models.* J Biomed Mater Res A, 2009. **88**(4): p. 858-71.
86. Friedl, P., et al., *New dimensions in cell migration.* Nat Rev Mol Cell Biol, 2012. **13**(11): p. 743-747.
87. Lasfargues, E.Y., *Cultivation and behavior in vitro of the normal mammary epithelium of the adult mouse. II. Observations on the secretory activity.* Exp Cell Res, 1957. **13**(3): p. 553-62.
88. Astashkina, A.I., et al., *A 3-D organoid kidney culture model engineered for high-throughput nephrotoxicity assays.* Biomaterials, 2012. **33**(18): p. 4700-11.

89. Astashkina, A., *Organoid kidney tubule culture for drug toxicity screening.* The University of Utah). ProQuest Dissertations and Theses,, 2012. **207.**
90. Petrini, P., et al., *Design, synthesis and properties of polyurethane hydrogels for tissue engineering.* J Mater Sci Mater Med, 2003. **14**(8): p. 683-6.
91. Kleinman, H.K. and G.R. Martin, *Matrigel: Basement membrane matrix with biological activity.* Seminars in Cancer Biology, 2005. **15**(5): p. 378-386.
92. Lee, K.Y. and D.J. Mooney, *Alginate: properties and biomedical applications.* Prog Polym Sci, 2012. **37**(1): p. 106-126.
93. Kuo, C.K. and P.X. Ma, *Ionically crosslinked alginate hydrogels as scaffolds for tissue engineering: part 1. Structure, gelation rate and mechanical properties.* Biomaterials, 2001. **22**(6): p. 511-21.
94. Kuo, C.K. and P.X. Ma, *Ionically crosslinked alginate hydrogels as scaffolds for tissue engineering: Part 1. Structure, gelation rate and mechanical properties.* Biomaterials, 2001. **22**(6): p. 511-521.
95. Di Lullo, G.A., et al., *Mapping the ligand-binding sites and disease-associated mutations on the most abundant protein in the human, type I collagen.* Journal of Biological Chemistry, 2002. **277**(6): p. 4223-4231.
96. Prockop, D.J. and K.I. Kivirikko, *Collagens: molecular biology, diseases, and potentials for therapy.* Annu Rev Biochem, 1995. **64**: p. 403-34.
97. Gross, J. and D. Kirk, *The heat precipitation of collagen from neutral salt solutions: some rate-regulating factors.* Journal of Biological Chemistry, 1958. **233**(2): p. 355-60.
98. Schor, S.L., *Cell proliferation and migration on collagen substrata in vitro.* J Cell Sci, 1980. **41**: p. 159-75.
99. Schor, S.L., T.D. Allen, and B. Winn, *Lymphocyte migration into three-dimensional collagen matrices: a quantitative study.* J Cell Biol, 1983. **96**(4): p. 1089-96.
100. Schor, S.L., T.D. Allen, and C.J. Harrison, *Cell migration through three-dimensional gels of native collagen fibres: collagenolytic activity is not required for the migration of two permanent cell lines.* J Cell Sci, 1980. **46**: p. 171-86.
101. Gowans, J.L., *The recirculation of lymphocytes from blood to lymph in the rat.* J Physiol, 1959. **146**(1): p. 54-69.
102. Miller, E.J., *The collagens of the extracellular matrix.* Soc Gen Physiol Ser, 1977. **32**: p. 71-86.
103. Ivanoff, A., et al., *Infiltrative capacity of T leukemia cell lines: a distinct functional property coupled to expression of matrix metalloproteinase-9 (MMP-9) and tissue inhibitor of metalloproteinases-1 (TIMP-1).* Clin Exp Metastasis, 1999. **17**(8): p. 695-711.
104. Wolf, K., et al., *Amoeboid shape change and contact guidance: T-lymphocyte crawling through fibrillar collagen is independent of matrix remodeling by MMPs and other proteases.* Blood, 2003. **102**(9): p. 3262-3269.
105. Ivanoff, J., T. Talme, and K.G. Sundqvist, *The role of chemokines and extracellular matrix components in the migration of T lymphocytes into three-dimensional substrata.* Immunology, 2005. **114**(1): p. 53-62.
106. Sundqvist, K.G., et al., *T lymphocyte infiltration of two- and three-dimensional collagen substrata by an adhesive mechanism.* Exp Cell Res, 1993. **206**(1): p. 100-10.

107. Shimazu, K., et al., *Morphogenesis of MDCK cells in a collagen gel matrix culture under stromal adipocyte-epithelial cell interaction.* Kidney international, 2001. **60**(2): p. 568-578.
108. Pampaloni, F., et al., *Madin-Darby canine kidney cells are increased in aerobic glycolysis when cultured on flat and stiff collagen-coated surfaces rather than in physiological 3-D cultures.* Proteomics, 2010. **10**(19): p. 3394-413.
109. Inoue, C.N., et al., *Reconstruction of tubular structures in three-dimensional collagen gel culture using proximal tubular epithelial cells voided in human urine.* In Vitro Cell Dev Biol Anim, 2003. **39**(8-9): p. 364-7.
110. Nichol, J.W., et al., *Cell-laden microengineered gelatin methacrylate hydrogels.* Biomaterials, 2010. **31**(21): p. 5536-44.
111. Lee, K.C. and I.B. Koh, *Intravascular tumour targeting of aclarubicin-loaded gelatin microspheres. Preparation, biocompatibility and biodegradability.* Archives of Pharmacal Research, 1987. **10**(1): p. 42-49.
112. Ratcliffe, J., et al., *Preparation and evaluation of biodegradable polymeric systems for the intra-articular delivery of drugs.* Journal of pharmacy and pharmacology, 1984. **36**(7): p. 431-436.
113. Van Den Bulcke, A.I., et al., *Structural and rheological properties of methacrylamide modified gelatin hydrogels.* Biomacromolecules, 2000. **1**(1): p. 31-38.
114. Benton, J.A., et al., *Photocrosslinking of gelatin macromers to synthesize porous hydrogels that promote valvular interstitial cell function.* Tissue Engineering Part A, 2009. **15**(11): p. 3221-3230.
115. Schuurman, W., et al., *Gelatin-Methacrylamide Hydrogels as Potential Biomaterials for Fabrication of Tissue-Engineered Cartilage Constructs.* Macromol Biosci, 2013.
116. Amundson, D., et al., *Practicing internal medicine onboard the USNS COMFORT in the aftermath of the Haitian earthquake.* Ann Intern Med, 2010. **152**(11): p. 733-7.
117. Hughes, C.S., L.M. Postovit, and G.A. Lajoie, *Matrigel: a complex protein mixture required for optimal growth of cell culture.* Proteomics, 2010. **10**(9): p. 1886-90.
118. Gao, X., et al., *Basic structure and cell culture condition of a bioartificial renal tubule on chip towards a cell-based separation microdevice.* Anal Sci, 2011. **27**(9): p. 907-12.
119. Krause, S., et al., *A novel 3D in vitro culture model to study stromal-epithelial interactions in the mammary gland.* Tissue Eng Part C Methods, 2008. **14**(3): p. 261-71.
120. Subramanian, B., et al., *Tissue-engineered three-dimensional in vitro models for normal and diseased kidney.* Tissue Engineering Part A, 2010. **16**(9): p. 2821-2831.
121. Hoppensack, A., et al., *A human in vitro model that mimics the renal proximal tubule.* Tissue Engineering Part C: Methods, 2014.
122. Glynne, P. and T. Evans, *Inflammatory cytokines induce apoptotic and necrotic cell shedding from human proximal tubular epithelial cell monolayers.* Kidney international, 1999. **55**(6): p. 2573-2597.
123. Beltman, J.B., A.F. Marée, and R.J. de Boer, *Analysing immune cell migration.* Nature Reviews Immunology, 2009. **9**(11): p. 789-798.

124. Wolf, K., et al., *Compensation mechanism in tumor cell migration mesenchymal–amoeboid transition after blocking of pericellular proteolysis.* The Journal of cell biology, 2003. **160**(2): p. 267-277.
125. Pampaloni, F., et al., *Madin–Darby canine kidney cells are increased in aerobic glycolysis when cultured on flat and stiff collagen-coated surfaces rather than in physiological 3-D cultures.* Proteomics, 2010. **10**(19): p. 3394-3413.
126. Lee, K.Y. and D.J. Mooney, *Hydrogels for tissue engineering.* Chem Rev, 2001. **101**(7): p. 1869-79.
127. Van Den Bulcke, A.I., et al., *Structural and rheological properties of methacrylamide modified gelatin hydrogels.* Biomacromolecules, 2000. **1**(1): p. 31-8.
128. Australia, O. *Cell Voyager 1000*. Available from: http://www.olympusaustralia.com.au/Product/Detail/444/Cell-Voyager-1000.
129. Bakočević, N., et al., *T Cell–Dendritic Cell Interaction Dynamics during the Induction of Respiratory Tolerance and Immunity.* The Journal of Immunology, 2010. **184**(3): p. 1317-1327.
130. Ernandez, T. and T.N. Mayadas, *Immunoregulatory role of TNFalpha in inflammatory kidney diseases.* Kidney Int, 2009. **76**(3): p. 262-76.
131. Shankar, A., et al., *Markers of inflammation predict the long-term risk of developing chronic kidney disease: a population-based cohort study.* Kidney Int, 2011. **80**(11): p. 1231-1238.